

Supporting Information for

Separation of branched alkane feeds by a synergistic action of zeolite and metal-organic framework

Pedro F. Brântuas^a, Adriano Henrique^{a, b}, Mohammad Wahiduzzaman^c, Alexander von Wedelstedt^c, Tanmoy Maity^{a,d}, Alírio E. Rodrigues^b, Farid Nouar^e, U-Hwang Lee^f, Kyung-Ho Cho^f, Guillaume Maurin^{c, 3}, José A. C. Silva^{a, 2} and Christian Serre^{e, 1}

^a Centro de Investigação de Montanha (CIMO), Instituto Politécnico de Bragança, Campus de Santa Apolónia, 5300-253 Bragança, Portugal

^b Laboratory of Separation and Reaction Engineering - Laboratory of Catalysis and Materials (LSRE/LCM), Department of Chemical Engineering, Faculty of Engineering University of Porto, Rua Dr. Roberto Frias, S/N, 4200-465 Porto, Portugal

^c ICGM, Univ. Montpellier, CNRS, ENSCM, Montpellier, France

^d Present address : Tata Institute of Fundamental Research – Hyderabad, Hyderabad, Telangana 500046, India

^e Institut des Matériaux Poreux de Paris, ESPCI Paris, Ecole Normale Supérieure de Paris, CNRS, PSL University, 75005 Paris, France

^f Research Group for Nanocatalysts (RGN) and Chemical & Process Technology Division, Korea Research Institute of Chemical Technology (KRICT), Gajeong-Ro 141, Yuseong, Daejeon 34114, Republic of Korea

TABLE OF CONTENTS

LIST OF FIGURES	3
LIST OF TABLES	7
1. PREPARATION OF MATERIALS	8
1.1 Synthesis and characterization of powder MOF MIL-160(Al)	8
1.1.1. Powder X-Ray Diffraction	8
1.1.2. Infrared Spectroscopy	8
1.1.3. Thermogravimetric Analysis	9
1.1.4. Gas sorption study	9
1.2 Synthesis and characterization of shaped MOF MIL-160(Al)	9
1.3 Characterization of Zeolite 5A	9
2. SAMPLING OF MIL-160(Al).....	9
3. EXPERIMENTAL SETUP AND PROCEDURE	10
3.1 Experimental apparatus to measure breakthrough curves	10
3.2 Experimental apparatus to perform continuous cyclic experiments	11
3.3 Physical properties of the adsorption column and MFC's and syringe characteristics	13
3.4 Experimental procedure to measure breakthrough curves.....	13
4. PROCESS PERFORMANCE.....	14
4.1 Research Octane Number Calculations	14
4.2 Productivity.....	14
5. EXPERIMENTAL MEASUREMENTS	14
6. CONFIGURATION-BIAS MONTE CARLO SIMULATIONS	17
REFERENCES	72

LIST OF FIGURES

Figure S1. PXRD patterns of MIL-160(Al).....	18
Figure S2. FTIR spectra of MIL-160(Al).....	19
Figure S3. TGA analysis of MIL-160(Al).....	20
Figure S4. Nitrogen adsorption and desorption isotherms at 77 K on MIL-160(Al)	21
Figure S5. Pore size distribution and cumulative pore volume of MIL-160(Al).	22
Figure S6. Adsorbent materials in shaped form: a) MIL-160(Al) beads (2.0 to 3.35 mm). b) Zeolite 5A binder-free beads (1.2 to 2.0 mm).....	23
Figure S7. Experimental procedure for agglomeration of powdered samples of MIL-160(Al).....	24
Figure S8. Schematic diagram of the experimental apparatus used to measure single and multicomponent breakthrough curves. (AC) adsorption column; (APC) advanced pneumatic control; (FID) flame ionization detector; (MFC) mass flow controller; (S/SP) split/splitless-injector; (SP) syringe pump; (TCD) thermal conductivity detector; (TL) transfer line; (V1) 4-way valve; (V2) and (V3) 6-way valve; (V4) 3-way valve.	25
Figure S9. Schematic diagram of the experimental apparatus used to perform the continuous cyclic experiments: a) Gas preparation section for checking the paraffins vaporization; b) Pressurization with feed and adsorption; and c) Vacuum countercurrent depressurization with inert He purge desorption. Blue and green lines represent the paraffins (adsorption) and He purge (desorption) flow paths inside the system, respectively.....	26
Figure S10. Adsorption columns used on the sorption experiments.	27
Figure S11. Experimental multicomponent breakthrough curves for an equimolar quinary mixture of C6 isomers on powder MIL-160 at 373 K and a) 10 kPa, b) 25.0 kPa, and c) 50kPa.	28
Figure S12. Experimental multicomponent breakthrough curves for an equimolar quinary mixture of C6 isomers on powder MIL-160 at 423 K and a) 10 kPa and b) 25 kPa.....	29
Figure S13. Experimental multicomponent breakthrough curves for an equimolar quinary mixture of C6 isomers on powder MIL-160 at 473 K and a) 10 kPa, b) 25.0 kPa, and c) 50kPa.	30
Figure S14. Experimental quinary adsorption equilibrium isotherms for an equimolar mixture of C6 isomers on powder MIL-160 at (a) 373 K, (b) 423 K, and (c) 473 K.	31
Figure S15. Experimental multicomponent breakthrough curves for an equimolar quinary mixture of C6 isomers on powder CAU-10 at 423 K and 50kPa.....	32
Figure S16. Experimental multicomponent breakthrough curves for an equimolar septenary mixture of C5/C6 isomers on powder MIL-160 at 50 kPa and a) 373 K and b) 473 K.	33
Figure S17. Experimental multicomponent breakthrough curves for an equimolar quinary mixture of branched C5/C6 isomers on powder MIL-160 at 50 kPa and a) 373 K and b) 473 K.....	34

Figure S18. Experimental pure component adsorption equilibrium isotherms of C5/C6 isomers on shaped MIL-160(Al). a) iC5, b) nC5, c) 22DMB, d) 23DMB, e) 3MP, f) 3MP, and g) nC6 at 373 K (squares), 423K (circles), and 473 K (diamonds).....	35
Figure S19. Experimental multicomponent breakthrough curves for an equimolar binary mixture of C6 isomers on shaped MIL-160 at 423 K and 50 kPa. a) 22DMB/23DMB, b) 23DMB/2MP, c) 3MP/2MP, and d) 2MP/nC6.....	36
Figure S20. Experimental multicomponent breakthrough curves for an equimolar ternary mixture of C6 isomers on shaped MIL-160 at 423 K and 50 kPa. a) 22DMB/2MP/nC6 and b) 23DMB/2MP/nC6.....	37
Figure S21. Experimental multicomponent breakthrough curves for an equimolar quinary mixture of C6 isomers on shaped MIL-160 at 50 kPa and a) 423 K and b) 473 K.....	38
Figure S22. Experimental multicomponent breakthrough curves for a septenary mixture of pentane and hexane isomers on shaped MIL-160 at 423 K and 50 kPa. The concentration used is equal to one reported by Holcombe et al. ⁵ , which corresponds to the composition of the product stream from an isomerization reactor.	39
Figure S23. Experimental multicomponent breakthrough curves for a quinary mixture of pentane and hexane isomers on shaped MIL-160 at 423 K and 50 kPa. The concentration used is equal to one reported by Holcombe et al. ⁵ , which corresponds to the composition of the product stream from an isomerization reactor, considering the branched isomers as the only paraffins in the mixture.....	40
Figure S24. Experimental multicomponent breakthrough curves for an equimolar septenary mixture of C6 isomers in a mixed bed of shaped MOF MIL-160(Al) (70 wt%) and binder-free beads Zeolite 5A (30 wt%) at 473 K and 50 kPa.	41
Figure S25. Experimental preliminary PSA test for an equimolar septenary mixture of C5/C6 isomers in a mixed bed of shaped MOF MIL-160(Al) (70%) and binder-free beads Zeolite 5A (30 wt%) at 473 K and 50.0 kPa. Steady-state effluent concentration.....	42
Figure S26. Molecular representation of the pentane/hexane isomers. Implicit hydrogen atoms are lumped onto the neighboring carbons and described with pseudo atoms CH3, CH2, CH and C according to TraPPE-UA potentials.	43
Figure S27. Simulated single component adsorption isotherms of hexane isomers in MIL-160 for the (a) pristine and (b) and 5° linker rotation obtained at 423 K.	44
Figure S28. CBMC simulated co-adsorption isotherms of equimolar n-C6/2MP binary mixture for the MIL-160 with 5° tilted linkers at $T = 423$ K (left panel) and a snapshot of the adsorbed nC6 (green spheres) and 2MP (purple spheres) molecules at $P = 0.1$ bar within the channel of the MOF (right panel).	45
Figure S29. CBMC simulated co-adsorption isotherms of equimolar 2MP/3MP binary mixture for the MIL-160 with 5° tilted linkers at $T = 423$ K (left panel) and a snapshot of the adsorbed 2MP (green	

spheres) and 3MP (purple spheres) molecules at $P = 0.1$ bar within the channel of the MOF (right panel).	46
Figure S30. CBMC simulated co-adsorption isotherms of equimolar 2MP/23DMB binary mixture for the MIL-160 with 5° tilted linkers at $T = 423$ K (left panel) and a snapshot of the adsorbed 2MP (green spheres) and 23DMB (purple spheres) molecules at $P = 0.1$ bar within the channel of the MOF (right panel).	47
Figure S31. CBMC simulated co-adsorption isotherms of equimolar 22DMB/23DMB binary mixture for the MIL-160 with 5° tilted linkers at $T = 423$ K (left panel) and a snapshot of the adsorbed 22DMB (green spheres) and 23DMB (purple spheres) molecules at $P = 0.1$ bar within the channel of the MOF (right panel).	48
Figure S32. Intermolecular radial pair distribution functions of the (a) CH3(UA), (b) CH2(UA), (c) CH(UA) and (d) C of the hexane isomers with respect to MIL-160 framework atoms in the vicinity of the pore channel calculated for an equimolar quinary mixture at $T = 423$ K and $P = 0.1$ bar.	49
Figure S33. Illustration of a typical spatial arrangement and van der Waals close contacts (<3.5 Å) of a <i>n</i> -C6 molecule with the MIL-160 pore walls taken from a representative adsorption snapshot derived from CBMC simulation performed for an equimolar quinary mixture of all C6 isomers at $T = 423$ K and $P = 0.2$ bar.	50
Figure S34. Illustration of a typical spatial arrangement and van der Waals close contacts (<3.5 Å) of a 2MP molecule with the MIL-160 pore walls taken from a representative adsorption snapshot derived from CBMC simulation performed for an equimolar quinary mixture of all C6 isomers at $T = 423$ K and $P = 0.2$ bar.	51
Figure S35. Illustration of a typical spatial arrangement and van der Waals close contacts (<3.5 Å) of a 23DMB molecule with the MIL-160 pore walls taken from a representative adsorption snapshot derived from CBMC simulation performed for an equimolar quinary mixture of all C6 isomers at $T = 423$ K and $P = 0.2$ bar.	52
Figure S36. Illustration of CBMC simulated pore filling and spatial arrangement of all C5 and C6 isomers in the MOF channel obtained for an equimolar septenary mixture of C5/6 isomers at $P = 0.2$ bar and $T = 423$ K. Color codes: nC5 (orange spheres), iC5 (black spheres), nC6 (yellow spheres), 2MP (cyan spheres), 3MP (purple spheres), 23DMB (green spheres) and 22DMB (blue spheres), MOF framework atoms: Al (pink), Carbon (grey) and Oxygen (red), hydrogen atoms are omitted for clarity.	53
Figure S37. Illustration of a typical spatial arrangement and van der Waals close contacts (<3.5 Å) of a iC5 molecule with the MIL-160 pore walls taken from a representative adsorption snapshot derived from CBMC simulation performed for an equimolar septenary mixture of all C5 and C6 isomers at $T = 423$ K and $P = 0.2$ bar.	54

Figure S38. Illustration of a typical spatial arrangement and van der Waals close contacts (<3.5 Å) of a <i>n</i> -C5 molecule with the MIL-160 pore walls taken from a representative adsorption snapshot derived from CBMC simulation performed for an equimolar septenary mixture of all C5 and C6 isomers at $T = 423$ K and $P = 0.2$ bar.....	55
Figure S39. CBMC simulated co-adsorption isotherms of equimolar iC5/2MP/3MP/23DMB/22DMB mixture for the MIL-160 with 5° tilted linkers at $T = 423$ K.....	56

LIST OF TABLES

Table S1. Textural properties of MIL-160(Al).....	57
Table S2. Column, MFC's, and syringe characteristics for the experimental studies.....	58
Table S3. Molecular dimensions and research octane numbers of C5 and C6 alkanes.....	59
Table S4. Experimental conditions to measure multicomponent breakthrough curves for an equimolar quinary mixture of C6 isomers on powder MIL-160(Al)	60
Table S5. Experimental conditions to measure multicomponent breakthrough curves for an equimolar quinary mixture of hexane isomers on powder CAU-10(Al)	61
Table S6. Experimental conditions to measure multicomponent breakthrough curves for an equimolar quinary/septenary mixture of C5/C6 isomers on powder MIL-160(Al).....	62
Table S7. Experimental conditions to measure pure component breakthrough curves of C6 isomers on shaped MIL-160(Al).....	63
Table S8. Experimental conditions to measure multicomponent breakthrough curves for an equimolar binary/ternary mixture of C6 on shaped MIL-160(Al).....	64
Table S9. Experimental conditions to measure multicomponent breakthrough curves for an equimolar quinary mixture of C6 isomers on shaped MIL-160(Al).....	65
Table S10. Experimental conditions to measure multicomponent breakthrough curves for a septenary mixture of C5/C6 isomers on shaped MIL-160(Al) with an isomerization concentration ¹⁶	66
Table S11. Experimental conditions to measure multicomponent breakthrough curves for an equimolar septenary mixture of C5/C6 isomers in a mixed bed of shaped MOF MIL-160(Al) (70 wt%) and binder-free beads Zeolite 5A (30 wt%).....	67
Table S12. Experimental conditions for preliminary PSA tests for an equimolar septenary mixture of C5/C6 isomers in a mixed bed of shaped MOF MIL-160(Al) (70 wt%) and binder-free beads Zeolite 5A (30 wt%).	68
Table S13. Intermolecular LJ-potential parameters for the C5 and C6 isomers.....	69
Table S14. Intermolecular LJ Potential parameters for the MIL-160(Al) framework atoms.....	70
Table S15. Henry's constants (K_H) of hexane and pentane isomers in MIL-160(Al) at 423 K	71

1. PREPARATION OF MATERIALS

1.1 Synthesis and characterization of powder MOF MIL-160(Al)

The synthesis parameters for MIL-160(Al) were adapted from previously reported conditions¹: 1.2 g (7.5 mmol) of 2-furandicarboxylic acid and 1.17 g (7.5 mmol) of Al(OH)(CH₃COO)₂ were mixed with 15 mL of distilled water and then subject to reflux at 383 K for 24 hours. After cooling to room temperature, the solid material was collected by filtration, washed with ethanol and dried in a vacuum oven.

For the characterization of MIL-160(Al) several physico-chemical measurements were performed: powder x-ray diffraction (PXRD), Fourier transformed infrared spectroscopy (FTIR), thermogravimetric analysis (TGA), and gas adsorption study to understand their porous nature. The PXRD patterns of the samples were recorded with a Bruker D8 ADVANCE diffractometer using Cu K α radiation ($\lambda = 1.5418 \text{ \AA}$). FTIR spectra were measured on a Perkin-Elmer Spectrum 100 spectrometer under ATR technique. Thermogravimetric analysis was performed on a Mettler Toledo TGA2 unit under O₂ atmosphere at 3 K.min⁻¹ rate. Nitrogen adsorption isotherms at 77 K and pressure range of 0 – 10⁵ Pa were measured using a micromeritics TriStar II Plus gas sorption system. A sample of ~ 50 mg material was introduced into an analysis tube and were evacuated under dynamic vacuum at desired temperature using micromeritics Smart VacPrep high vacuum pump. Prior to the sorption experiments, the samples were out gassed at the desired temperature (423 K) for 6 h under vacuum. The Horvath-Kawazoe method (Slit Pore Geometry) was applied to evaluate the pore sizes distribution of the samples.

1.1.1. Powder X-Ray Diffraction

The powder x-ray diffraction patterns of MIL-160(Al) are illustrated in Figure S1 clearly showing that the sample synthesized corresponds to MIL-160(Al). Comparison of synthesized materials (blue) with calculated powder pattern (red, extract from .cif) suggest that the purity and quality of MIL-160(Al) are very good and also match with reported pattern¹.

1.1.2. Infrared Spectroscopy

Fourier transformed infrared spectroscopy of materials are shown in Figure S2. FTIR spectra of both linker (FDCA) and MIL-160 reveals that there is no presence of unreacted acid linker in the MOF sample.

1.1.3. Thermogravimetric Analysis

Figure S3 reveals the thermogravimetric analysis under oxygen atmosphere of MIL-160 (heating rate of 3 K/min). The TG measurements show an initial 27% mass loss up to 373 K. This corresponds to adsorbed solvents and water molecules within the pores of the MOF. After that, the material is stable up to 573 K and then degrades. These results are well matched with the reported curve¹.

1.1.4. Gas sorption study

Gas sorption measurements were undertaken to understand the porous nature of MIL-160 synthesized materials. Figure S4 shows the N₂ adsorption and desorption isotherms at 77 K on MIL-160 (outgassed at 423 K under secondary vacuum for 6 hours), while Figure S5 exhibits the pore size distribution and cumulative pore volume. As can be seen, the N₂ adsorption isotherms are of type I according to the IUPAC classification², which is a signature characteristic of microporous materials. Brunauer Emmett Teller (BET) model was used for surface area calculation, being the data reported on Table S1. Textural properties of MIL-160(Al).Table S1, which also shows the average pore diameter, and maximum pore volume.

1.2 Synthesis and characterization of shaped MOF MIL-160(Al)

The shaping procedure is detailed in the patent WO 2016/186454 A1 filled by the Korea Research Institute of Chemical Technology (KRICT)³ with the result being shown in Figure S6a.

1.3 Characterization of Zeolite 5A

The binder-free beads of zeolite 5A were supplied by Chemiewerk Bad Koestritz GmbH (Germany), which consist of spherical particles with a diameter size ranging from 1.2 to 2.0 mm as can be seen in Figure S6b.

2. SAMPLING OF MIL-160(AL)

Prior to screening studies, powdered MIL-160 material was transformed into small agglomerates to minimize diffusion issues. The experimental procedure is described in Figure S7. First, the powdered solids were compacted into tablets in a manual hydraulic press machine (GS15011, Specac); the pressure

applied was 6.5 kg mm². Subsequently, the tablets were broken into small fragments and sieved to produce a known particle size distribution of around 2.5 mm.

3. EXPERIMENTAL SETUP AND PROCEDURE

3.1 Experimental apparatus to measure breakthrough curves

The equilibrium adsorption of C5 and C6 isomers in MIL-160(Al) were assessed in an apparatus developed to measure fixed-bed single and multicomponent breakthrough curves in the vapor phase, as shown in Figure S8. It mainly comprises two gas chromatographs (GC's, YL 6500, YL Instruments Co., Ltd.), with one being preparative and the other being analytic. Both GC's have a shockproof design and stable structure against oven temperature changes. The experimental setup consists of three main sections: (i) gas preparation, (ii) adsorption, and (iii) analytical section.

In the gas preparation section, the carrier gas helium (99.9996%, Linde) and the paraffins are introduced into the system. Helium is used as a carrier gas due to its inertness and enters the system in four different streams: the lines (1), (2), make up, and (8). The first three lines are directed to the preparative chromatograph, and line (8) is sent to the analytical part. The lines (1) and (2) are monitored by the mass flow controller (MFC, Alicat Scientific) while the make-up and line (8) pass through an advanced pneumatic control system (APC). The hydrocarbon stream is continuously introduced (in liquid phase) with a syringe pump (SP, Legato® 100, KD Scientific) in the carrier gas flowing in the line (1) to run into the inner heating region in a packed column inlet located in the preparative chromatograph.

The adsorption section consists of a stainless-steel column entirely filled with the adsorbent material and operated inside the preparative chromatograph oven. The stream from the packed column inlet runs into the switching 4-ports (V1) and 6-ports valve (V2, VICI, Valco Instruments Co.), bypassing the adsorption column. Simultaneously, the pure helium flowing in line 2, which also passes through these two valves, goes to the adsorption column via line 5. The column bypass is incorporated to check if the paraffins vaporization is stable with a constant concentration in the Thermal Conductivity Detector (TCD), while the make-up line is used to dilute the signal of the paraffins. When the concentration reaches a constant signal, the experiment can be started. Therefore, the 3-way ball valve (V4, SS-41GXS1, Swagelok) is directed to vent manually, and when the inert baseline is reached in the TCD (pure helium signal), the V1 valve is actuated, allowing the paraffins to run through the adsorption column. The transfer line which connects the preparative to the analytic GC is thermally controlled by a microcomputer-based digital temperature indicating controller (TL, ACS-13A, Shinko) to keep the

temperature stable and avoid any condensation of the gases from the preparative to the analytic chromatograph.

In the analytical section, used only for multicomponent experiments, the effluent flowing in the transfer line runs into a sampling 6-ports valve (V3, VICI, Valco Instruments Co.) inside the analytic chromatograph. In a pre-defined time interval, this valve sends an aliquot of gas to a capillary column (CC, with a 15 m length, 0.1 mm outside diameter, and 0.1 μ m poly(dimethyl sulfoxane) coating, Supelco), via line (9) by the pure helium stream coming from the line (8). Before entering the capillary column, the aliquot of gas passes through a split/splitless (S/SP) injector. The capillary column is immersed in an ice-water bath for better separation of component peaks. Finally, the capillary column output goes to the Flame Ionization Detector (FID) to be analyzed. This detector uses air (reconstituted air K with a concentration of 80% N₂ and 20% O₂, Linde) and hydrogen (99.9999%, Alpha Gaz) to produce its flame.

When the experiment finishes, i.e., the saturation state is reached, the paraffins injection by the syringe pump is cut, and the V1 valve is actuated. Then, the carrier gas flowing through line (2) performs the packed column desorption. After that, another experiment can be performed. Before the first RUN, the packed column, was activated for 12 h at 473 K under a pure helium flow. The helium lines corresponding to the reference side of TCD and split flow for the split/splitless injector (both controlled by the APC's modules) were omitted from Figure S8 for clarity.

The MFC's, SP, (V1, V2, and V3) VICI valves, and TF are connected to a laboratory power supply (230V AC) with a USB control module, which sends their digital data to a personal computer (PC) where they are automated. Oven temperatures, APC modules, and TCD and FID detectors are controlled and recorded using the YL-Clarity data acquisition software (YL Instruments Co., Ltd.), an intuitive chromatography data system with a user-friendly interface.

For the whole adsorption study, the hexanes isomers 22DMB/23DMB/nC₆ were supplied by Sigma Aldrich (> 99, 98, and 99%, respectively), 2MP by Alfa Aesar (> 99%), and 3MP by Acrōs Organics (> 99%); while the pentane isomers nC₅ by Riedel-de Haën (> 99%) and the iC₅ by Fluka (> 99%).

3.2 Experimental apparatus to perform continuous cyclic experiments

The continuous cyclic studies of preliminary PSA experiments on the zeolite 5A/MIL-160 mixed-bed were performed on the apparatus shown in Figure S9. The equipment was designed with the main characteristics of versatility and a wide range of operating conditions. As it can be seen, one adapted the

experimental setup previously showed to measure the adsorption equilibrium of C5/C6 isomers (Figure S8) to perform tests at a larger pilot level. The main differences consist on:

1 - A new oven (FD 53, Binder) assembled with an 8-ports valve (V3, VICI, Valco Instruments Co.) is incorporated in the system, in which the adsorption column is now operated. The oven is equipped with forced convection to promote a homogeneous temperature distribution, keeping the column in near-isothermal conditions. The V3 valve is used for switching between the adsorption and desorption steps of the cyclic experiment. This valve is also automated;

2 - The arrangement of the valves from the preparative chromatography was also modified. The V1 valve was rearranged in a way to switch between the by-pass of the adsorption column for checking the paraffins vaporization stability on the TCD detector (preliminary step of the experiment) and sending the hydrocarbon mixture to the column oven. The V2 valve, adapted to act as a 4-ports valve, is now in charge of directing the output of the packed column to the TCD detector and posterior analytical stage. All the lines between the column oven and the preparative GC are heat traced and insulated with ceramic wool and aluminum tape. The temperature of these lines is controlled by a temperature regulator (TR, HT-MC1, Horst GmbH);

3 - Two electronic high-speed pressure transducers (PT, PXM409-010BAUSBH, OMEGA) were installed in the packed column effluent lines (adsorption and desorption) to record the history of the pressure behavior during the pressurization and depressurization stages. The PT's are resistant to shock and vibrations and connects directly to the PC via USB, being the digital data recorded by the free OMEGA PC software;

4 - A diaphragm vacuum pump (VP, N810 Laboport, KNF) was also installed on the system to perform the depressurization of the packed column in the continuous cyclic experiments. Moreover, a flow metering valve (V4, SS-SS1-VH, Swagelok) was coupled to the vacuum pump to control the pressure in which the depressurization set point is stated. This valve operates manually.

The homemade apparatus developed to perform cyclic studies of a simplified 2 step PSA experiment with one single column is divided into three main sections: (i) gas preparation, (ii) adsorption (pressurization with feed + analysis), and (iii) desorption (vacuum countercurrent depressurization with inert He purge).

The gas preparation section is similar to the ones for the screening studies and is represented in Figure S9a. The carrier gas helium and the paraffins are introduced into the system, and the stability of this mixture vaporization should be checked. When the inert gas fills all the lines, the syringe pump starts to continuously introduce the hydrocarbons (in liquid phase) in the carrier gas from MFC to run through the vaporizer in the preparative chromatograph. Then, the vaporized mixture runs into the V1 valve,

mixes with the make-up line, and goes directly to the TCD detector. Simultaneously, the pure helium from the other MFC runs into the V3 valve, packed column, vacuum pump, V2 valve and goes to the preparative chromatograph's vent. When the vaporized mixture reaches a constant concentration, the V1 valve is actuated, and the mixture goes to the column oven, where the adsorption column will be operated and leaves the system by the vent line. A manual bubble flowmeter is used to check that the mixture is coming out from the system.

As soon as the paraffins mixture fills the line between the preparative and column oven (at this time, the inert baseline in the TCD (pure helium signal) is already reached), the adsorption section takes place, and the experiment can be started (Figure S9b). Therefore, the V3 valve is actuated. The adsorption column, mainly filled with He, is pressurized with the feed mixture. The pressure in the column rises from vacuum to atmospheric pressure. The feed mixture passes through the packed column, and a LRON enriched fraction is withdrawn through the product end. The output of the adsorption column goes back to the preparative chromatography, runs into the V2 valve, which is already in the position to send the mixture to the TCD, and flows through the transfer line to the analytical chromatography to evaluate its composition. The analytical procedure is the same as the ones described in section 0.

When the adsorption step finishes, the desorption stage occurs (Figure S9*Erreur ! Source du renvoi introuvable.c*). For that, both V3 and V2 valves are actuated. The column is then countercurrent depressurized with the vacuum pump and purged with a He stream. The effluent, mainly consisting of LRON molecules, is sent to the analytical section for chromatographic evaluation. Once the desorption time is up, another cycle can be started until reaching the cyclic steady state.

3.3 Physical properties of the adsorption column and MFC's and syringe characteristics

The sorption studies were performed with the MIL-160(Al) material in different forms and scales, being the experiments conducted on the agglomerates (originated from powdered form) in milligram scale, and in the form of shaped beads at gram scale. Consequently, the physical properties of the adsorption column and the specifications of MFC's controllers and syringes were chosen according to the operating conditions, as summarized in Table S2. The three different adsorption columns can be seen in Figure S10.

3.4 Experimental procedure to measure breakthrough curves

The experimental procedure to obtain single and multicomponent breakthrough curves consists of continuously measuring the concentration profile of the hydrocarbon species as a function of time at

the outlet of the adsorption column. Therefore, the packed bed is operated by introducing at the inlet the feed containing the adsorbable species diluted in a helium stream at a fixed total hydrocarbon pressure and temperature. The equilibrium loading (amount adsorbed) of the components is obtained by integrating the concentration profiles (molar rate history) of the breakthrough curves. Detailed information about the integrating procedure for multicomponent mixtures has already been reported elsewhere⁴.

4. PROCESS PERFORMANCE

4.1 Research Octane Number Calculations

The real-time RON of the hydrocarbon mixture leaving the adsorption column is calculated from the pure component RON_i values summarized in Table S3 averaged over the exit gas composition, as follows:

$$avg\ RON = \frac{\sum_{i=1}^n (y_i \times RON_i)}{\sum_{i=1}^n y_i}$$

where y_i is the molar fraction of the isomer i at the column outlet and n is the number of paraffins in the mixture.

4.2 Productivity

For the chosen set of thermodynamic conditions, a material balance over the adsorber gives information on the adsorbent productivity at a 92 RON, i.e., the number of moles product obtained per cubic decimeter of adsorbent. It should be noted that the value of 92 is obtained by averaging all isomers in the gas phase for the appropriate time interval. To calculate the volumetric productivity, the framework densities of 1.1184 and 0.9034 kg_{ads}.dm⁻³ were used for MIL-160(Al) in powdered and shaped form, respectively.

5. EXPERIMENTAL MEASUREMENTS

The adsorption behavior of pentane and hexane isomers in a fixed bed of MIL-160(Al) was investigated through a set of single and competitive breakthrough curves (binary, ternary, quinary, and septenary) performed at different temperatures and total hydrocarbon pressures relevant to the industrial

separation. Helium was used to set up a total pressure in the column of 101.3 kPa. The breakthrough curves are expressed in terms of the ratio of normalized molar $y_i y_{i0}^{-1}$ as a function of the total molar amount of paraffins fed to the column per unit mass adsorbent.

Figure S11, Figure S12, and Figure S13 show the breakthrough curves for an equimolar quinary mixture of all five hexane isomers in powder MIL-160(Al) at 373, 423, and 473 K, respectively. The effect of the total hydrocarbon pressure is shown in each figure: a) 10, b) 25, and c) 50 kPa. The experiment performed at 423 K and 50 kPa is presented in the main text (Figure 2). The corresponding quinary adsorption equilibrium isotherms obtained from these experiments are shown in Figure S14. Complete information on the experimental fixed bed runs performed is given in Table S4.

Figure S15 shows the multicomponent breakthrough curve for an equimolar quinary mixture of all five hexane isomers in powder CAU-10(Al), an isostructural form of MIL-160(Al), at 423 K and total hydrocarbon pressure of 50 kPa. Table S5 summarizes the experimental conditions applied.

Figure S16 shows the multicomponent breakthrough curves for an equimolar septenary mixture of pentanes and hexanes in powder MIL-160(Al) at 50.0 kPa. The effect of temperature is shown: a) 373 and b) 473 K. The experiment performed at 423 K is reported in the main text (Figure 5a). Table S6 summarizes the experimental conditions applied.

Figure S17 shows the multicomponent breakthrough curves for an equimolar quinary mixture of branched pentanes and hexane isomers in powder MIL-160(Al) at 50 kPa. The effect of temperature is shown: a) 373 and b) 473 K. The experiment performed at 423 K is reported in the main text (Figure 5b). The experimental conditions applied for these experiments are the same of those for the septenary mixtures shown in Table S6.

Figure S18 shows the pure component adsorption equilibrium isotherms of pentane and hexane isomers in shaped MIL-160(Al) at 373, 423, 473 K and hydrocarbon pressures ranging from 2.5 to 50 kPa. Table S7 summarizes the experimental conditions applied to measure the pure component breakthrough curves.

Figure S19 shows the breakthrough curves for an equimolar binary mixture of hexane isomers in shaped MIL-160 at 423 K and total hydrocarbon pressure of 50.0 kPa: a) 22DMB/23DMB, b) 23DMB/2MP, c) 3MP/2MP, and d) 2MP/nC6. Table S8 summarizes the experimental conditions applied.

Figure S20 shows the breakthrough curves for an equimolar ternary mixture of hexane isomers in shaped MIL-160 at 423 K and total hydrocarbon pressure of 50.0 kPa: a) 22DMB/2MP/nC6 and b) 23DMB/2MP/nC6. The experimental conditions applied for these experiments are the same of those for the binary mixtures shown in Table S8.

Figure S21 shows the multicomponent breakthrough curve for an equimolar quinary mixture of all hexane isomers in shaped MIL-160(Al) at 50 kPa. The effect of temperature is shown: a) 423 K and b) 473 K. Table S9 summarizes the experimental conditions applied.

Figure S22 shows the multicomponent breakthrough curves for a septenary mixture of branched pentane and hexane isomers in shaped MIL-160(Al) at 423 K and 50.0 kPa using a concentration reported by Holcombe et al. (1990)⁵, which corresponds to the composition of the product stream from an isomerization reactor, as indicated in Table S3. The experimental conditions for this experiment are shown in Table S10.

Figure S23 shows the multicomponent breakthrough curves for a quinary mixture of branched pentane and hexane isomers in shaped MIL-160(Al) at 423 K and 50.0 kPa, using a concentration reported by Holcombe et al. (1990)⁵, which corresponds to the composition of the product stream from an isomerization reactor, considering the branched isomers as the only paraffins in the mixture as indicated in Table S3. The experimental conditions for this experiment are those given in Table S10.

Figure S24 shows the multicomponent breakthrough curve for an equimolar septenary mixture of pentane and hexane isomers in a mixed bed of shaped MIL-160(Al) (70%)/ Zeolite 5A (30 wt%) at 473 K and 50 kPa. The experiment performed at 423 K is presented in the main text (Figure 6a). Table S11 summarizes the experimental conditions applied.

Figure S25 shows the preliminary PSA tests for an equimolar septenary mixture of pentane and hexane isomers in a mixed bed of shaped MIL-160(Al) (70%) and binder-free beads Zeolite 5A (30 wt%) at 473 K and 50 kPa. The experiment performed at 423 K is presented in the main text (Figure 6b). Table S12 summarizes the experimental conditions applied.

6. CONFIGURATION-BIAS MONTE CARLO SIMULATIONS

Configuration-bias Monte Carlo (CBMC) simulations were performed to calculate the adsorption isotherms of pure component and equimolar binary/quinary/septenary mixtures for pentane/hexanes isomers in MIL-160(Al) at 423 K. The crystal structure of MIL-160(Al) was taken from our previous study¹. Since the guest-induced reorientation of the linkers have been shown to impact the adsorption uptakes in MOF frameworks with small to moderate pore size⁶, CBMC calculations were first performed to assess the impact of the rotational flexibility of the furan linkers in MIL-160 framework on the pure component C6 adsorption isotherms. Figure S27 reveals that a 5° rotation of the furan along the two carboxylate C atoms leads to an overall fair agreement between the experimental and CBMC simulated adsorption hierarchy for the C6 isomers. Notably, this relatively small tilting that accounts a sub-angstrom level change in pore size (5.7 Å vs. 5.9 Å) yields same adsorption sequence — nC6 > 2MP > 3MP > 23DMB > 22DMB — observed in the pure component hexane isomers' adsorption measurements. The slight deviation between the experimental and simulated uptakes — particularly at higher pressure — can explain that a single configuration with identical tilting for all the linkers is likely unable to capture the whole adsorption regime. Importantly, the slopes of the simulated and experimental isotherms are in good agreement which led us to believe that further calculations on this tilted furan linker configuration of MIL-160 should provide reliable predictions on the multicomponent adsorption properties.

These CBMC simulations were performed with RASPA code⁷. We considered a simulation box made of 16 conventional unit cells ($2 \times 2 \times 4$) of the tilted MIL-160 configuration maintaining atoms at their initial positions. The interactions between the guest molecules and the MOF structure were described by a combination of site-to-site Lennard-Jones (LJ) potentials. Furthermore, van der Waals interactions were truncated at a cutoff distance of 12 Å. The Lennard-Jones cross-interaction parameters were calculated by means of the Lorentz-Berthelot mixing rules. Typically, 5×10^5 and 1×10^5 cycles (a cycle consist further 20 Monte Carlo moves) have been used for equilibration and production runs. These guest alkanes were modeled using the Transferable Potentials for Phase Equilibria United Atom (TraPPE-UA) models, i.e., molecules are represented by pseudo atoms: CH3, CH2, CH and C with implicit hydrogen atoms^{8,9}. The intramolecular C-C bond lengths of the molecules are set at 1.540 Å and the bond angles differ between 109.5° and 114°, depending on the bond type. The intermolecular LJ potential parameters are listed in Table S13. Atoms of the MOF framework were described by single LJ sites with parameters taken from the universal force field (UFF)¹⁰ except for the Al and H atoms for which the LJ interactions were neglected as previously reported¹. Henry's constant (K_H) for each of the pentane/hexanes was calculated using the revised Widom's test particle insertion method.

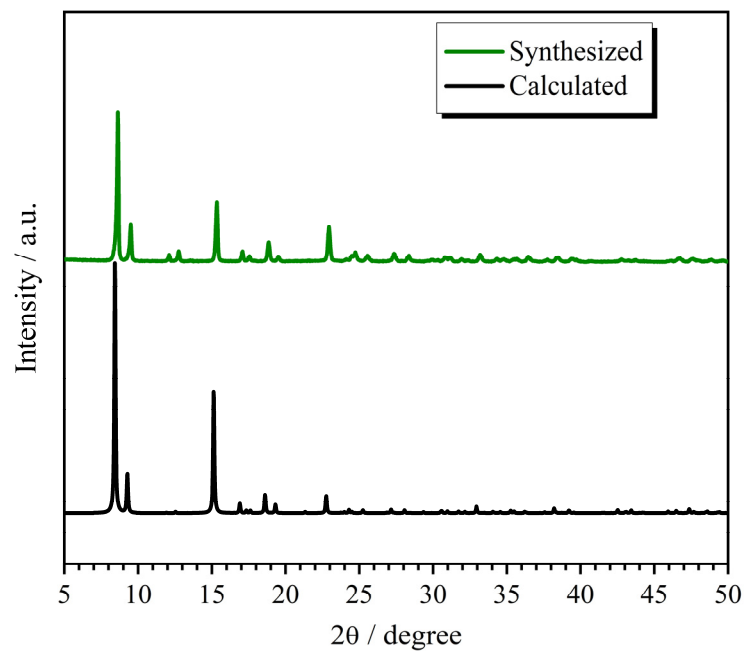


Figure S1. PXRD patterns of MIL-160(Al).

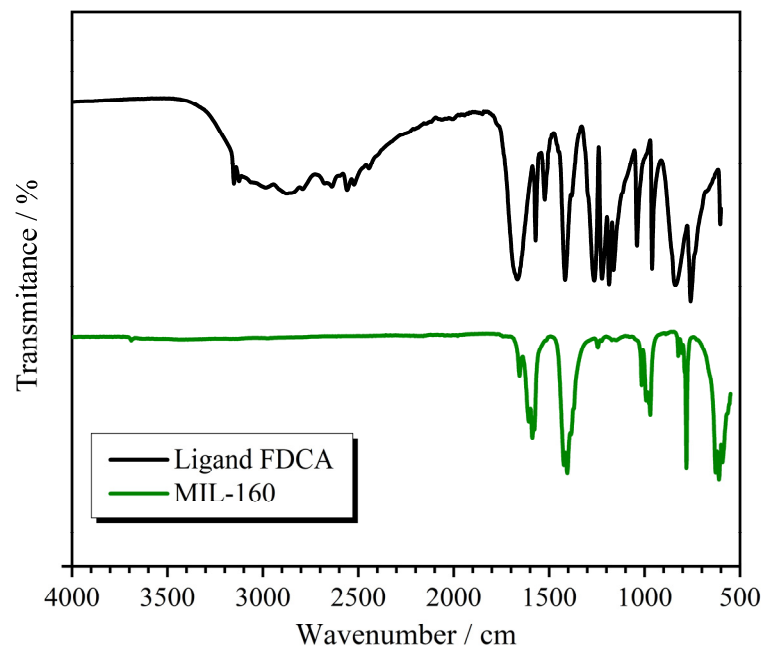


Figure S2. FTIR spectra of MIL-160(Al).

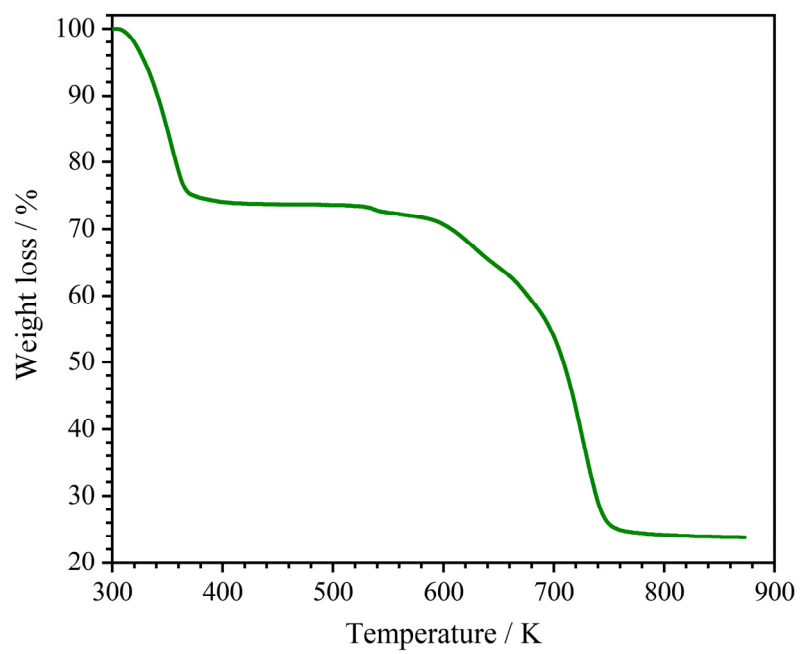


Figure S3. TGA analysis of MIL-160(Al).

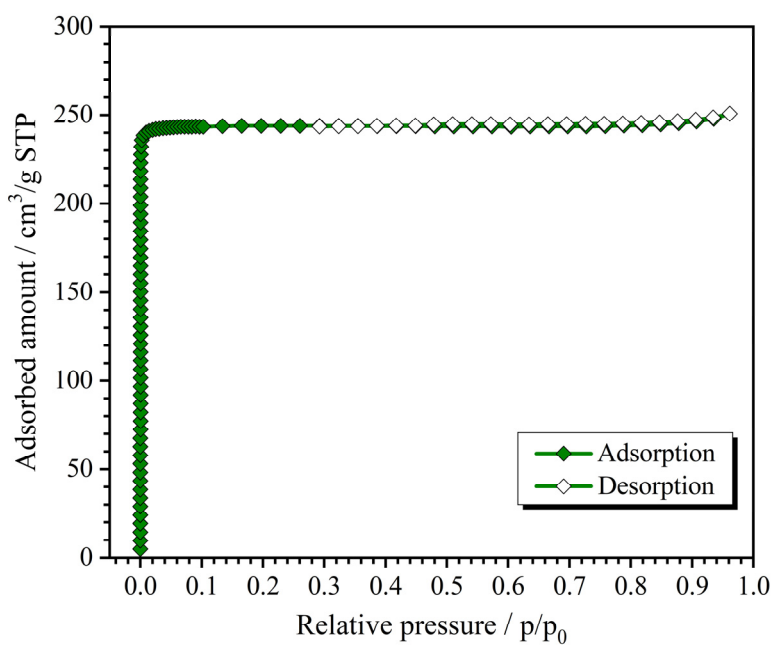


Figure S4. Nitrogen adsorption and desorption isotherms at 77 K on MIL-160(Al).

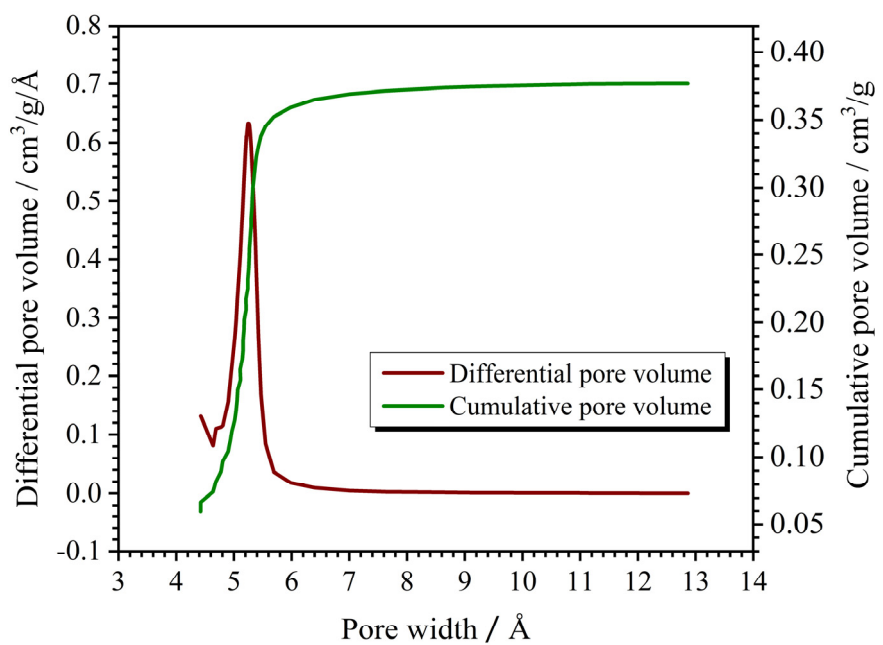


Figure S5. Pore size distribution and cumulative pore volume of MIL-160(Al).

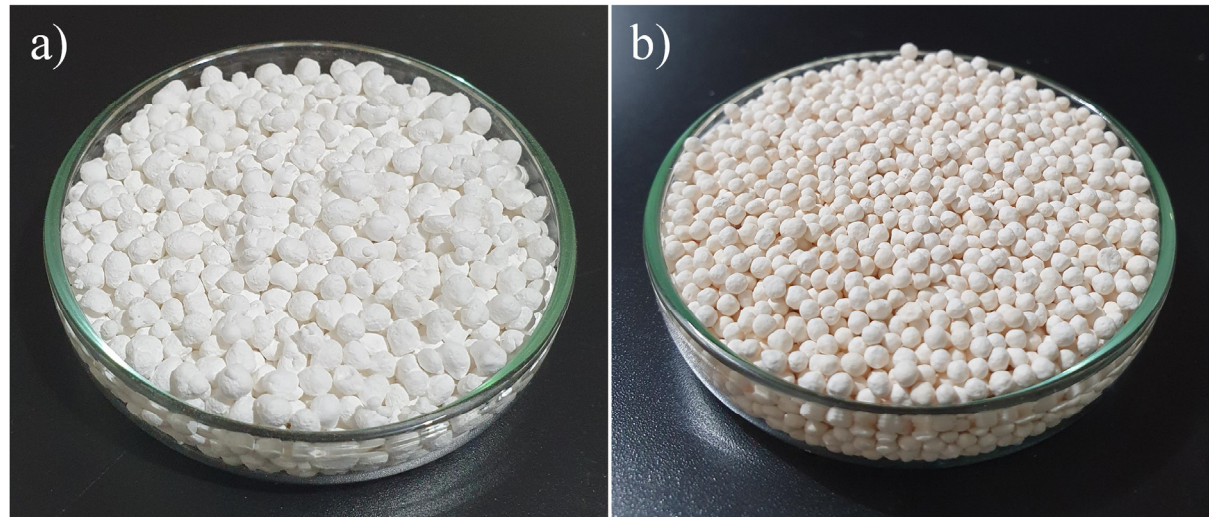


Figure S6. Adsorbent materials in shaped form: a) MIL-160(Al) beads (2.0 to 3.35 mm). b) Zeolite 5A binder-free beads (1.2 to 2.0 mm)

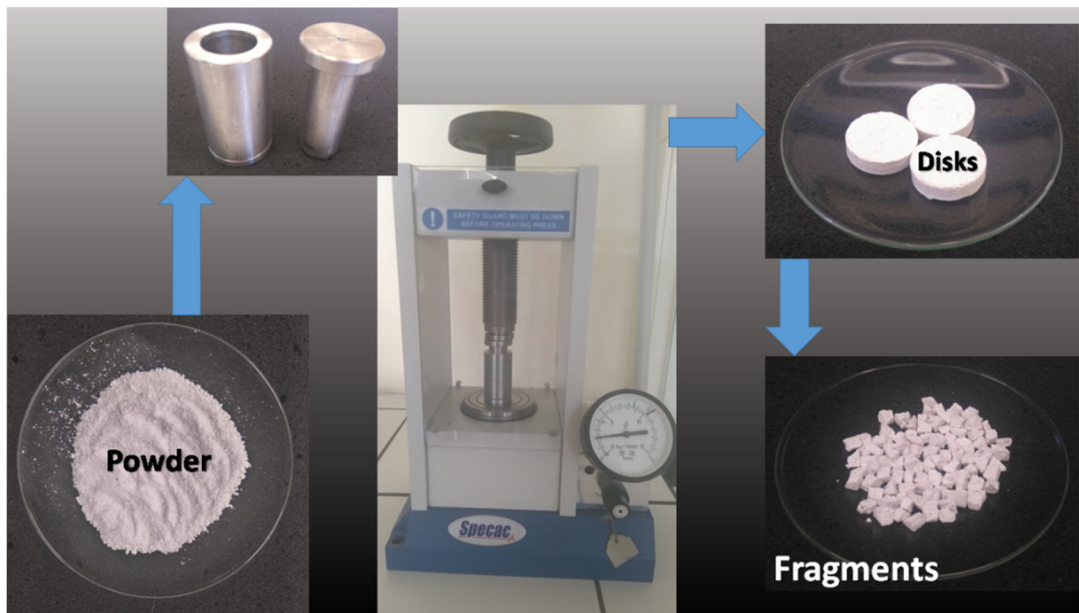


Figure S7. Experimental procedure for agglomeration of powdered samples of MIL-160(Al).

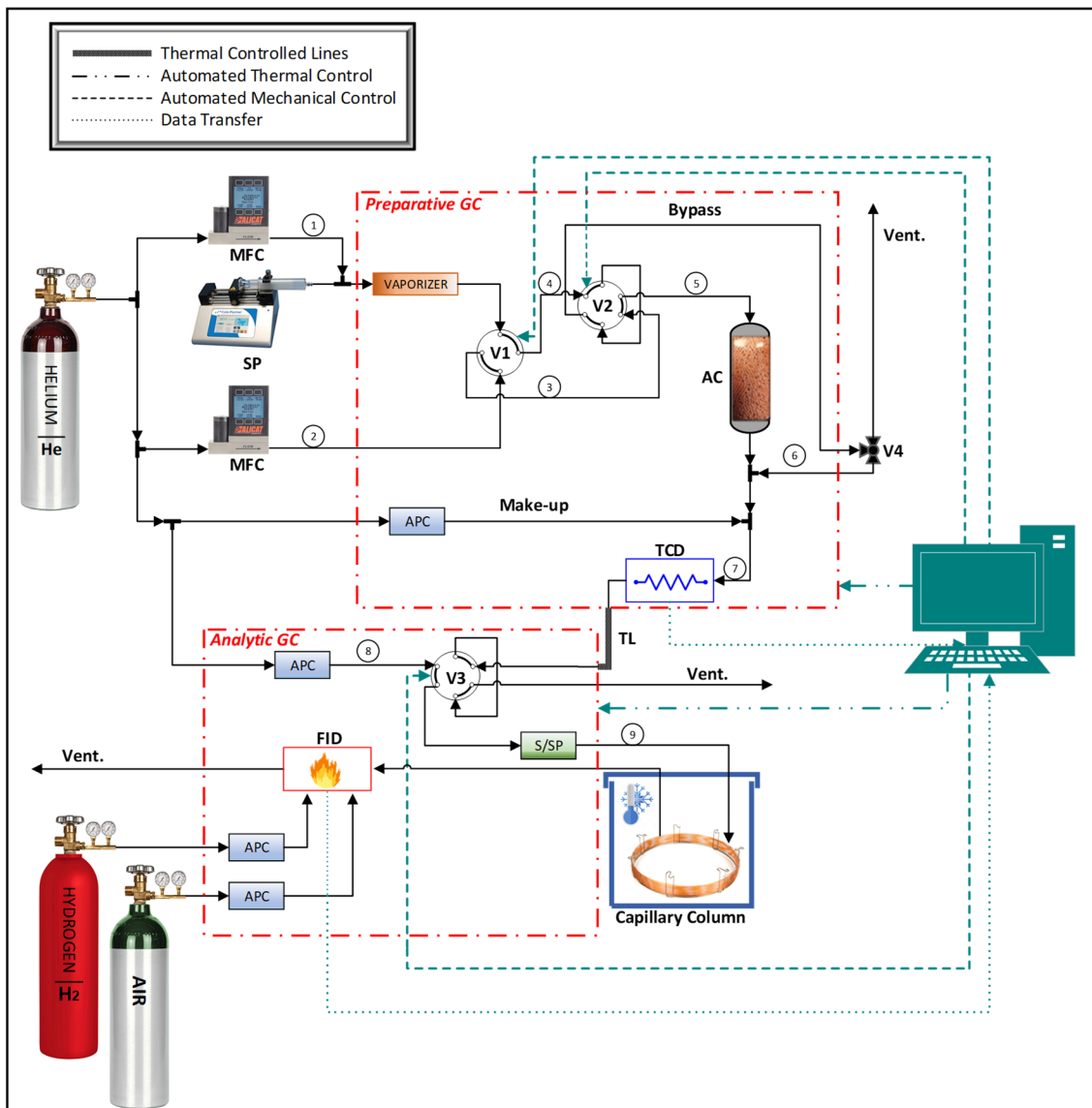


Figure S8. Schematic diagram of the experimental apparatus used to measure single and multicomponent breakthrough curves. (AC) adsorption column; (APC) advanced pneumatic control; (FID) flame ionization detector; (MFC) mass flow controller; (S/SP) split/splitless-injector; (SP) syringe pump; (TCD) thermal conductivity detector; (TL) transfer line; (V1) 4-way valve; (V2) and (V3) 6-way valve; (V4) 3-way valve.

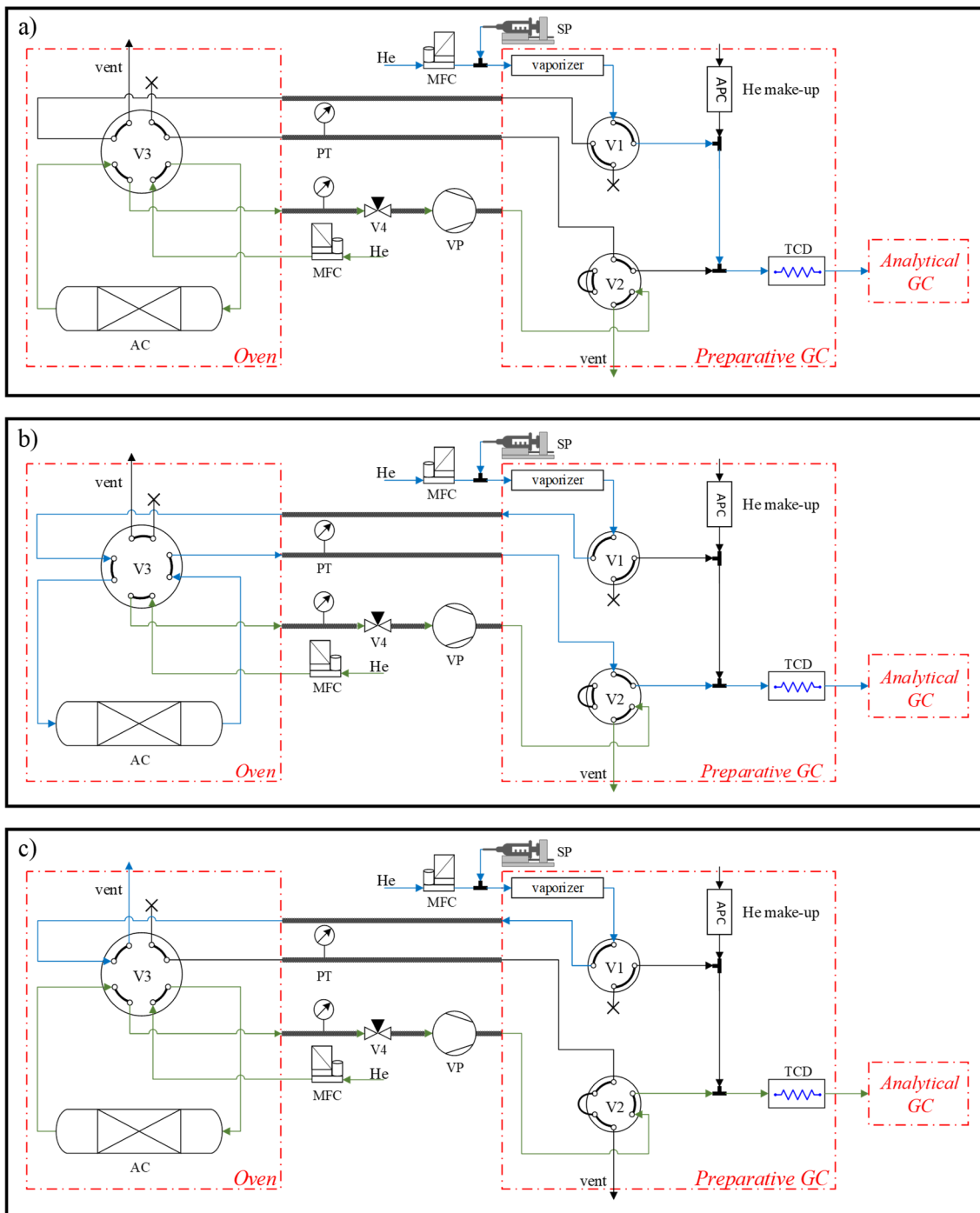


Figure S9. Schematic diagram of the experimental apparatus used to perform the continuous cyclic experiments: a) Gas preparation section for checking the paraffins vaporization; b) Pressurization with feed and adsorption; and c) Vacuum countercurrent depressurization with inert He purge desorption. Blue and green lines represent the paraffins (adsorption) and He purge (desorption) flow paths inside the system, respectively.

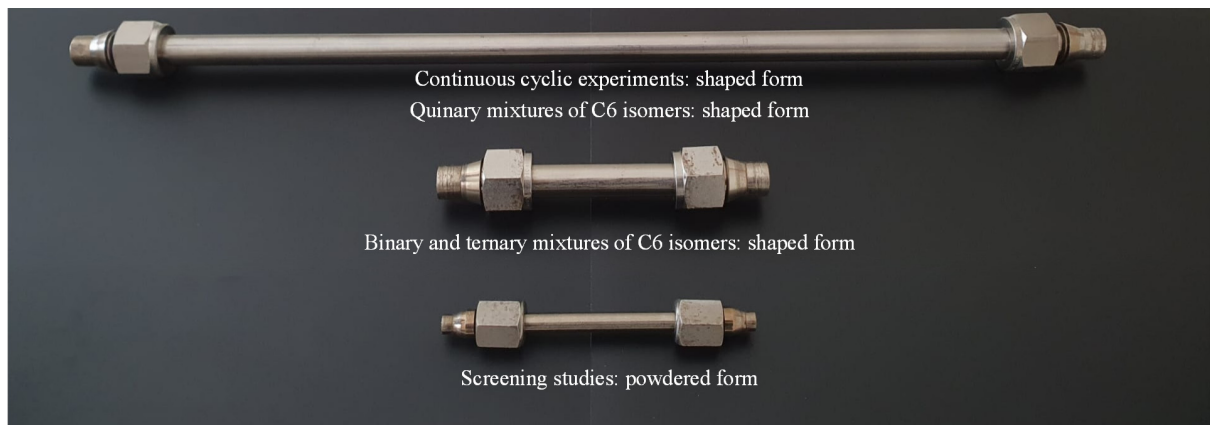


Figure S10. Adsorption columns used on the sorption experiments.

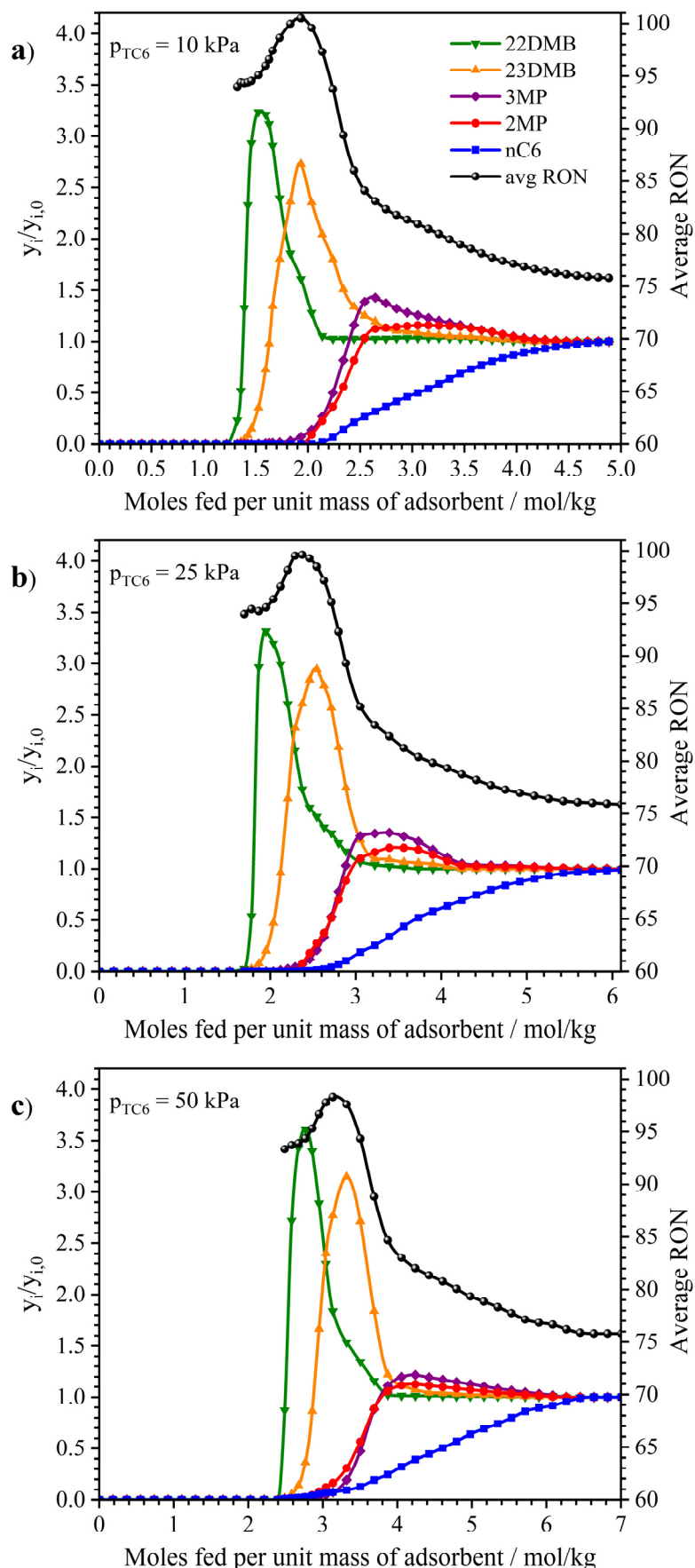


Figure S11. Experimental multicomponent breakthrough curves for an equimolar quinary mixture of C6 isomers on powder MIL-160 at 373 K and a) 10 kPa, b) 25.0 kPa, and c) 50 kPa.

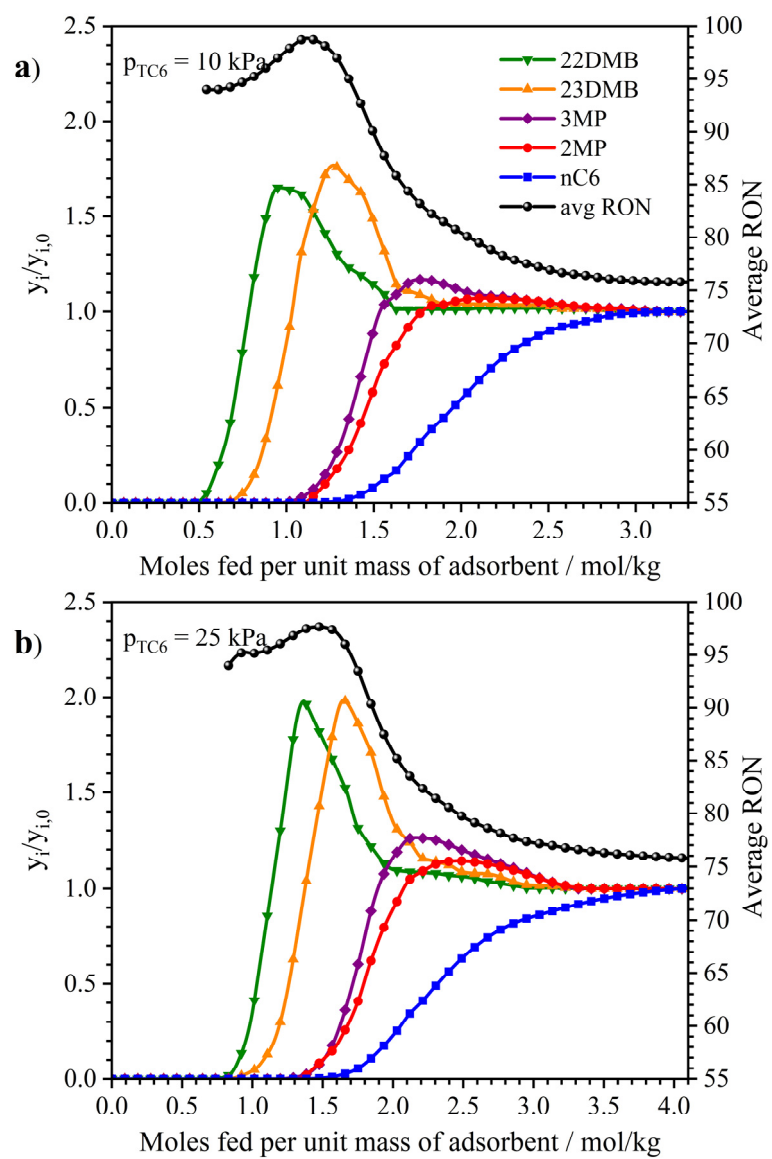


Figure S12. Experimental multicomponent breakthrough curves for an equimolar quinary mixture of C6 isomers on powder MIL-160 at 423 K and a) 10 kPa and b) 25 kPa.

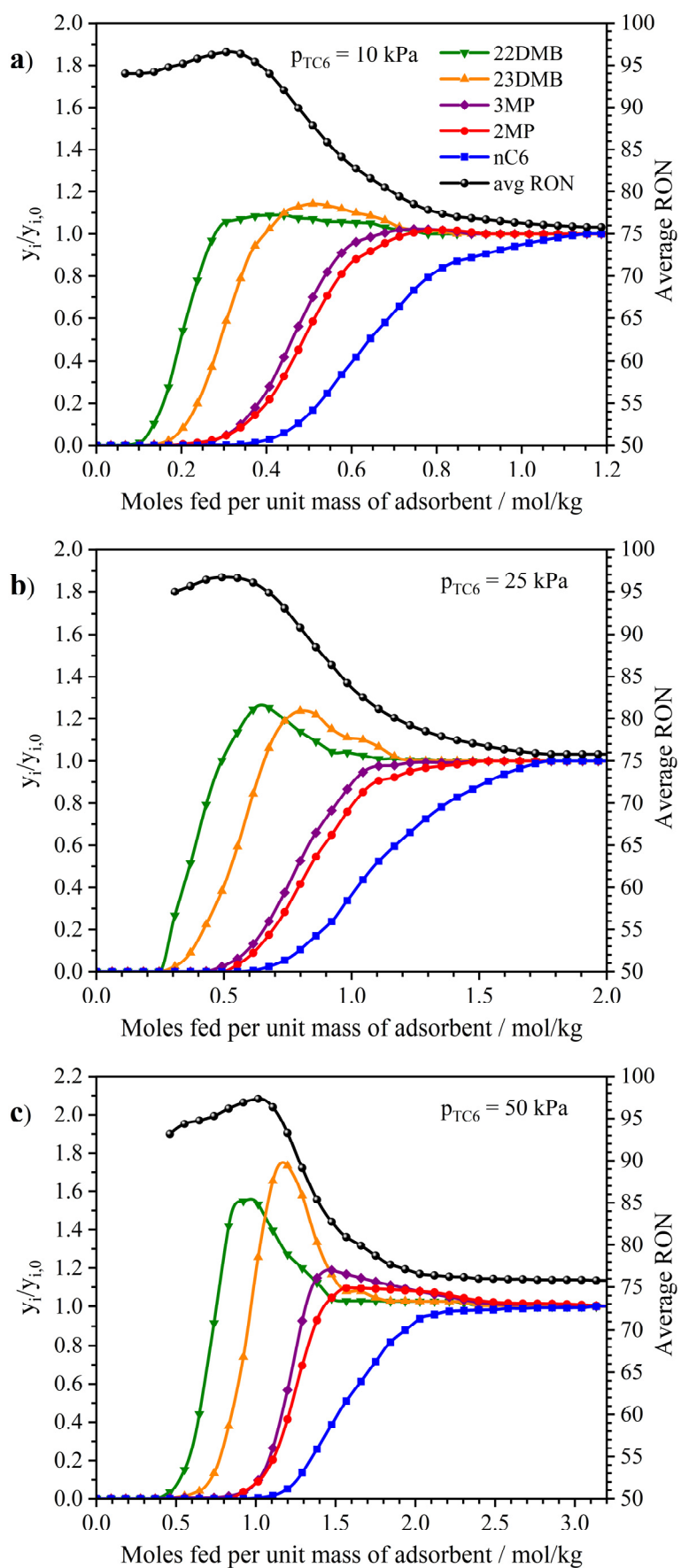


Figure S13. Experimental multicomponent breakthrough curves for an equimolar quinary mixture of C6 isomers on powder MIL-160 at 473 K and a) 10 kPa, b) 25.0 kPa, and c) 50 kPa.

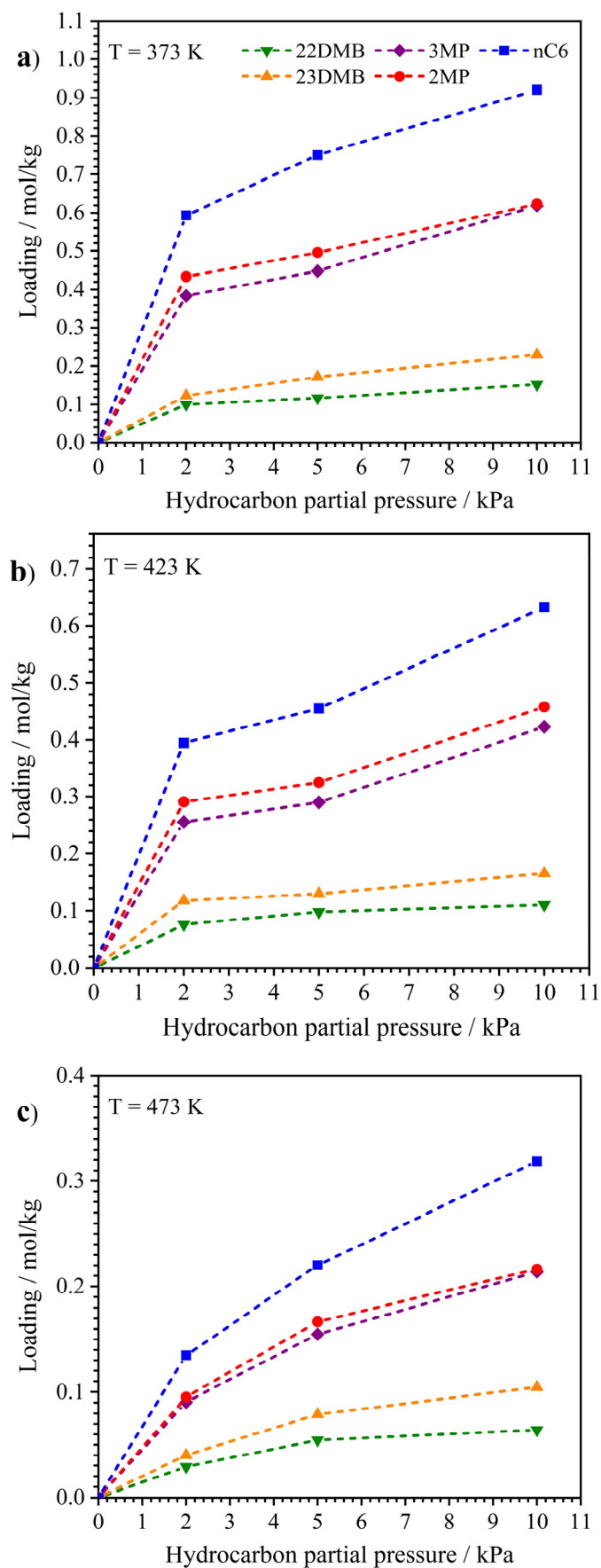


Figure S14. Experimental quinary adsorption equilibrium isotherms for an equimolar mixture of C6 isomers on powder MIL-160 at (a) 373 K, (b) 423 K, and (c) 473 K.

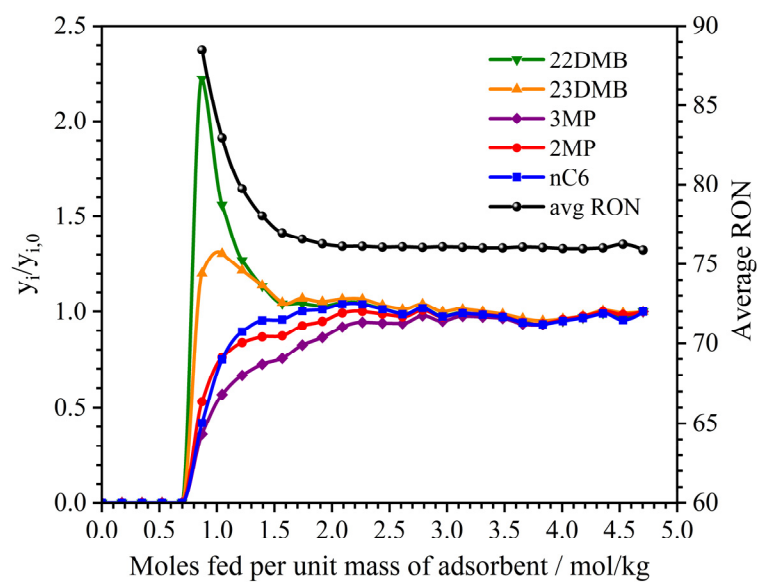


Figure S15. Experimental multicomponent breakthrough curves for an equimolar quinary mixture of C6 isomers on powder CAU-10 at 423 K and 50kPa.

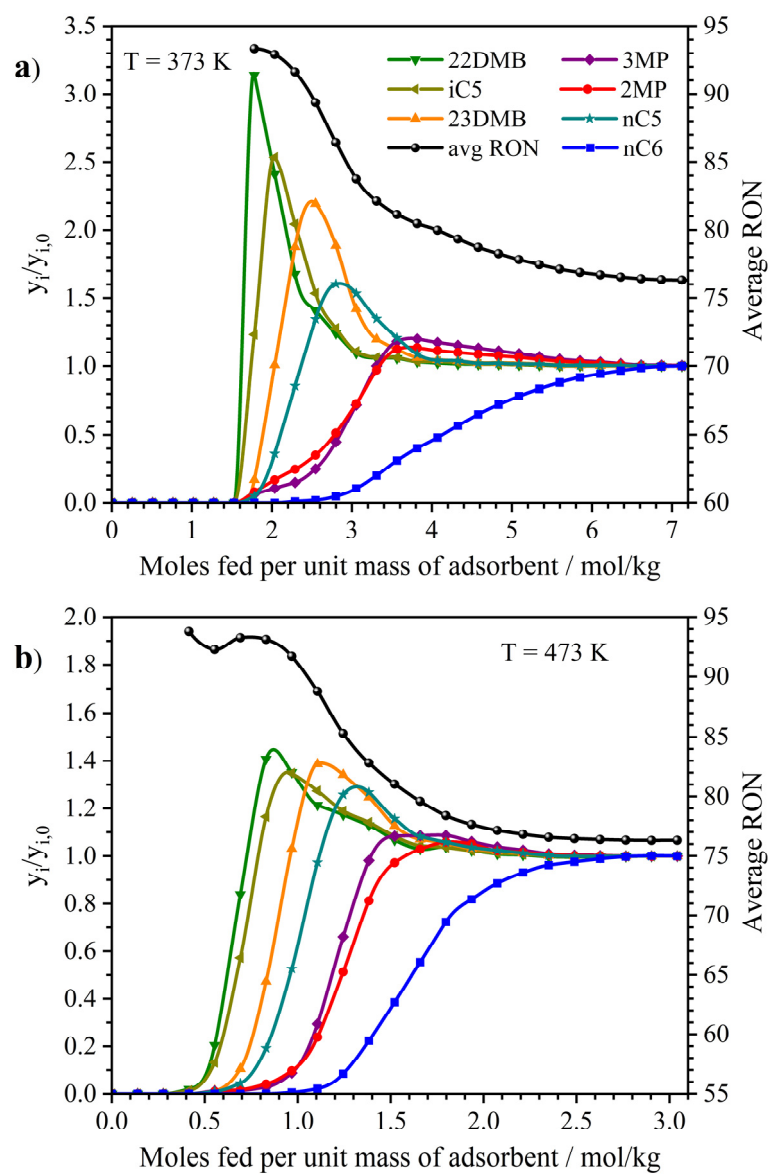


Figure S16. Experimental multicomponent breakthrough curves for an equimolar septenary mixture of C5/C6 isomers on powder MIL-160 at 50 kPa and a) 373 K and b) 473 K.

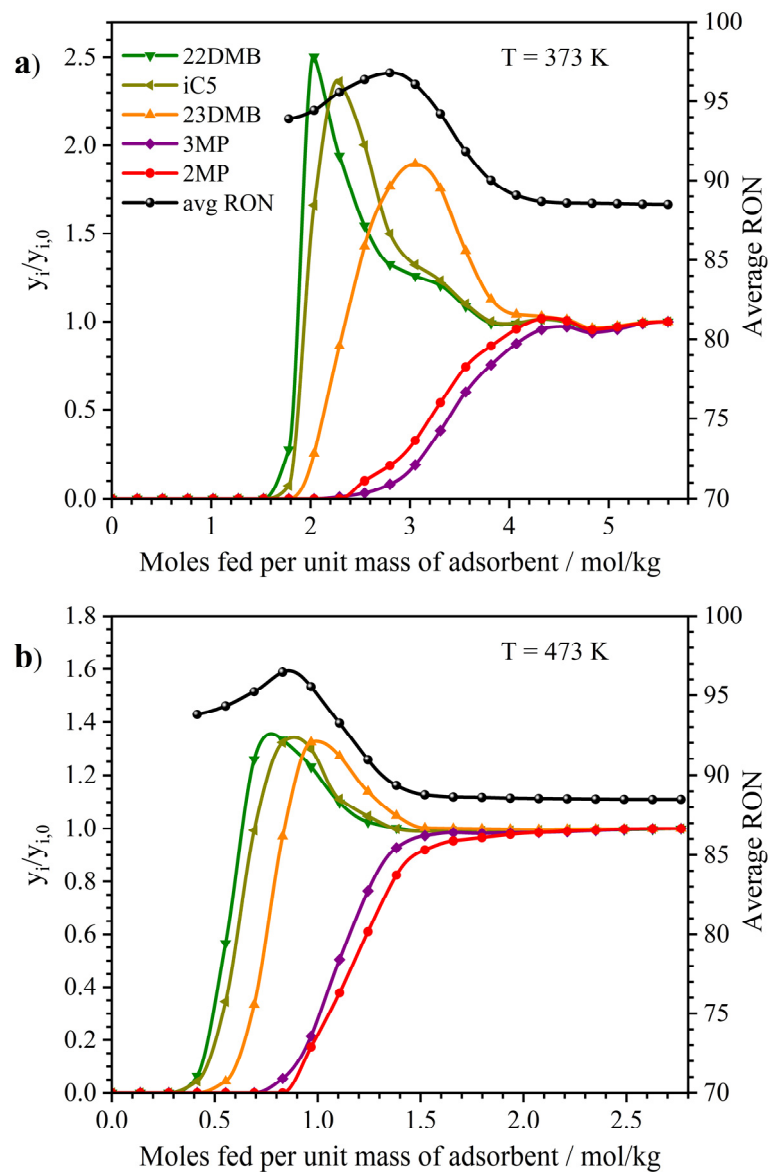


Figure S17. Experimental multicomponent breakthrough curves for an equimolar quinary mixture of branched C5/C6 isomers on powder MIL-160 at 50 kPa and a) 373 K and b) 473 K.

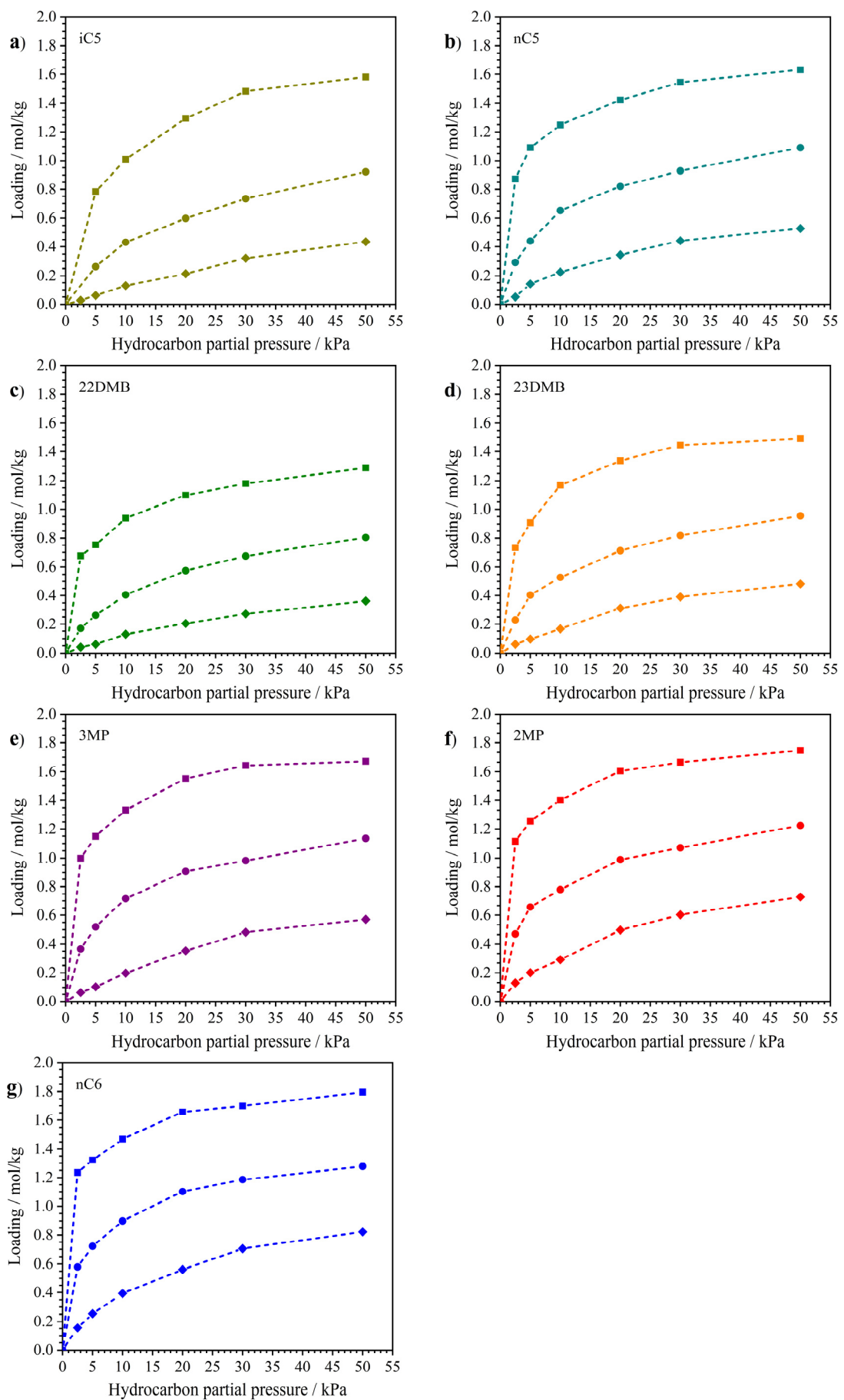


Figure S18. Experimental pure component adsorption equilibrium isotherms of C5/C6 isomers on shaped MIL-160(Al). a) iC5, b) nC5, c) 22DMB, d) 23DMB, e) 3MP, f) 3MP, and g) nC6 at 373 K (squares), 423K (circles), and 473 K (diamonds).

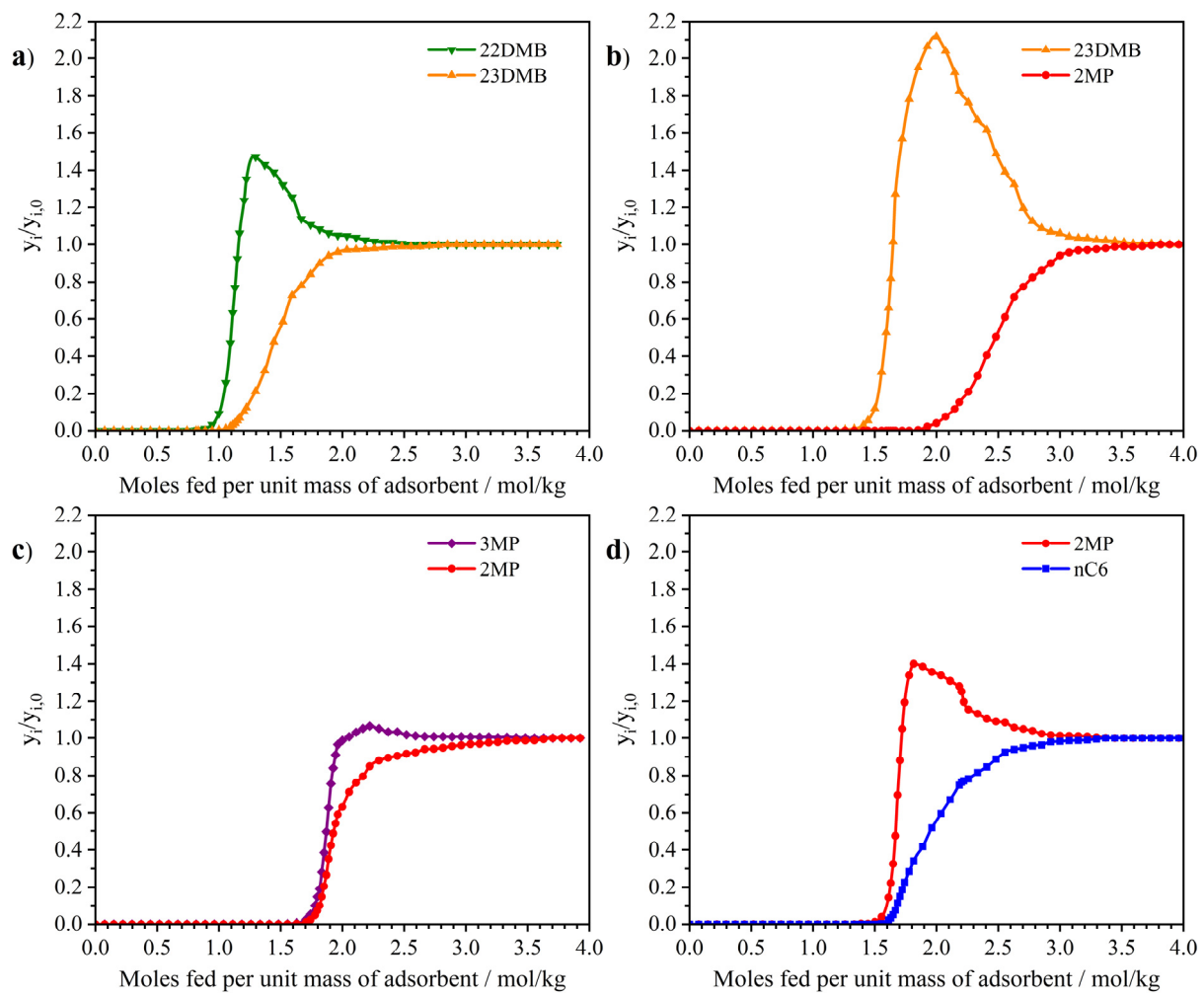


Figure S19. Experimental multicomponent breakthrough curves for an equimolar binary mixture of C6 isomers on shaped MIL-160 at 423 K and 50 kPa. a) 22DMB/23DMB, b) 23DMB/2MP, c) 3MP/2MP, and d) 2MP/nC6.

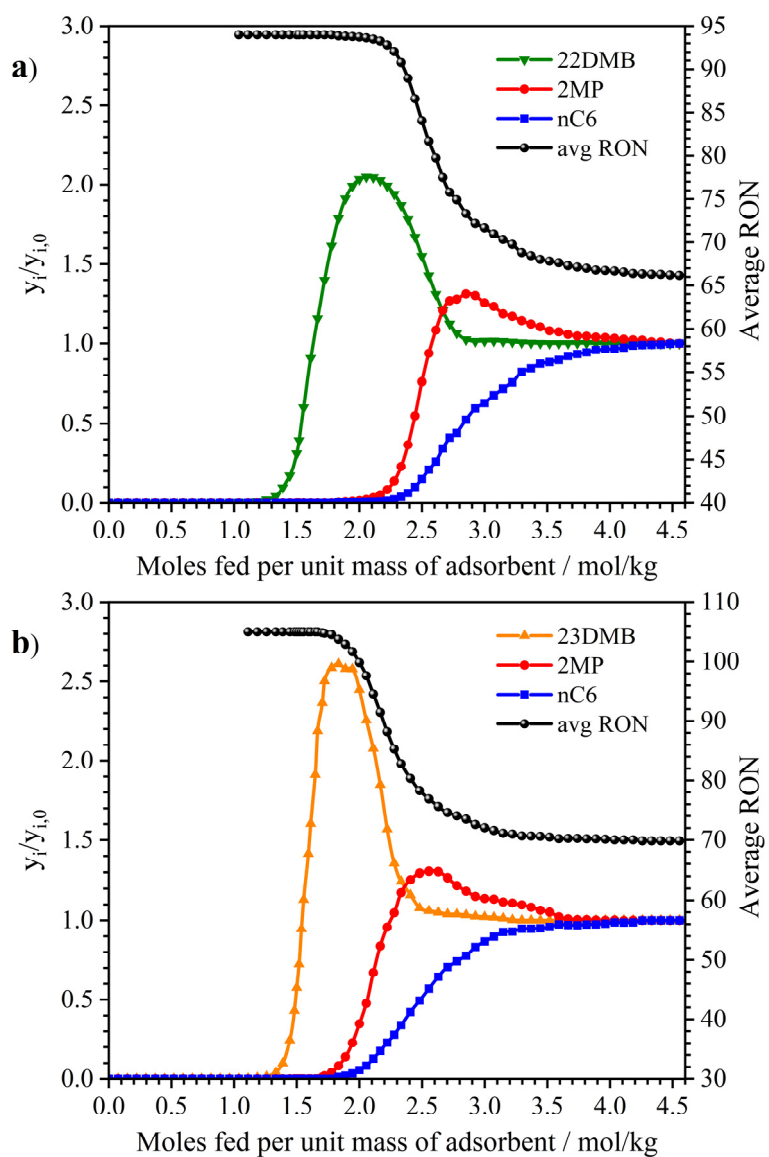


Figure S20. Experimental multicomponent breakthrough curves for an equimolar ternary mixture of C6 isomers on shaped MIL-160 at 423 K and 50 kPa. a) 22DMB/2MP/nC6 and b) 23DMB/2MP/nC6

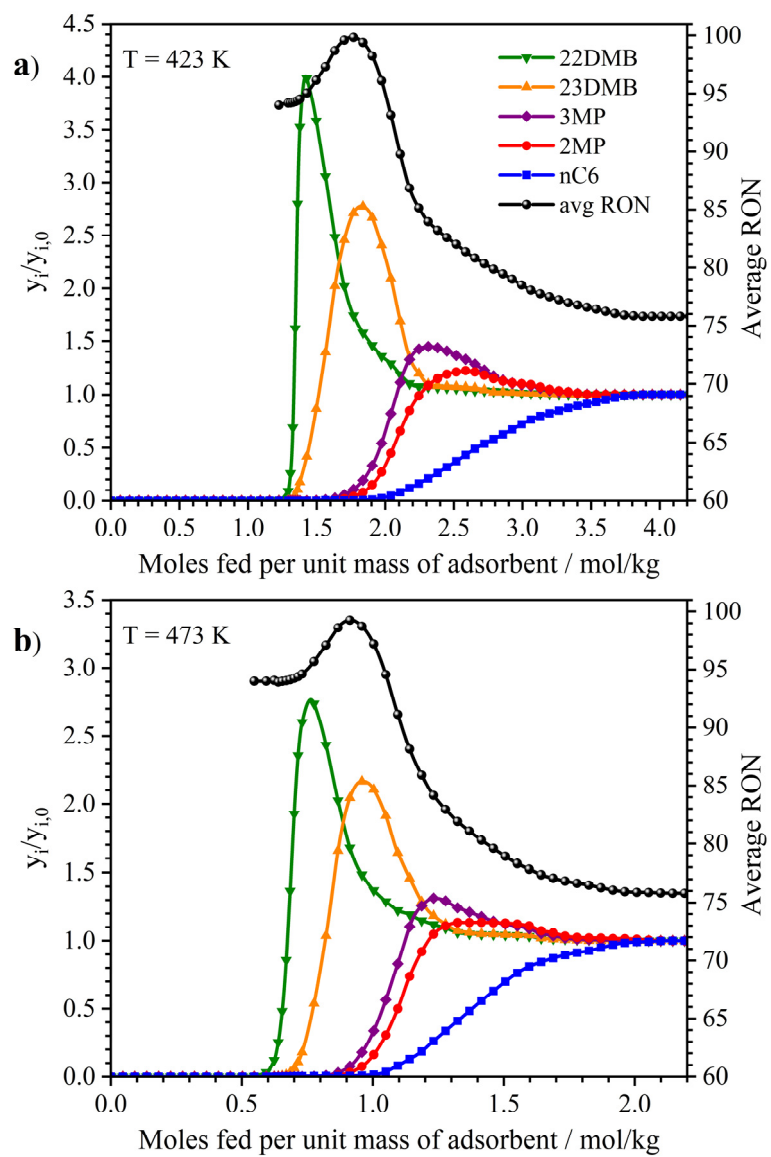


Figure S21. Experimental multicomponent breakthrough curves for an equimolar quinary mixture of C6 isomers on shaped MIL-160 at 50 kPa and a) 423 K and b) 473 K.

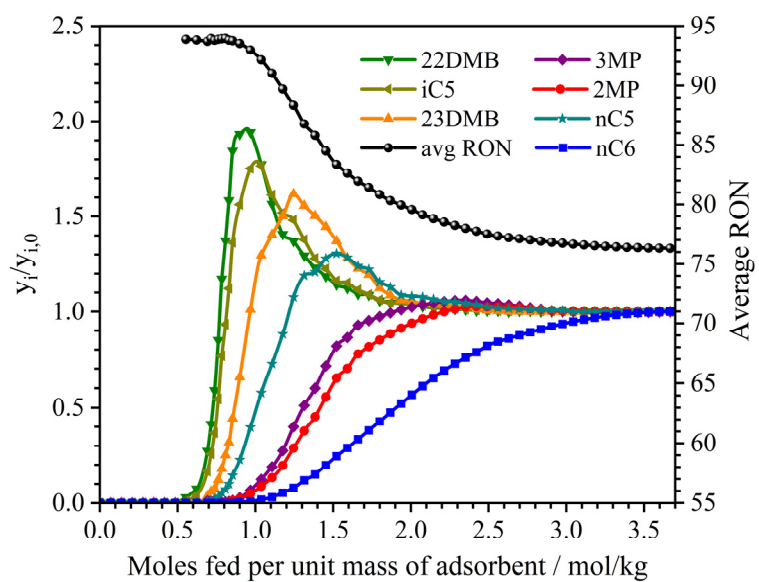


Figure S22. Experimental multicomponent breakthrough curves for a septenary mixture of pentane and hexane isomers on shaped MIL-160 at 423 K and 50 kPa. The concentration used is equal to one reported by Holcombe et al.⁵, which corresponds to the composition of the product stream from an isomerization reactor.

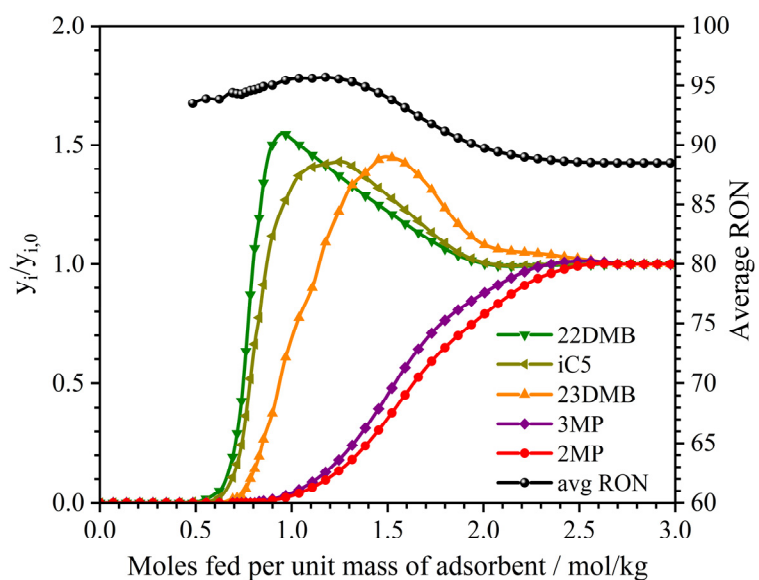


Figure S23. Experimental multicomponent breakthrough curves for a quinary mixture of pentane and hexane isomers on shaped MIL-160 at 423 K and 50 kPa. The concentration used is equal to one reported by Holcombe et al.⁵, which corresponds to the composition of the product stream from an isomerization reactor, considering the branched isomers as the only paraffins in the mixture

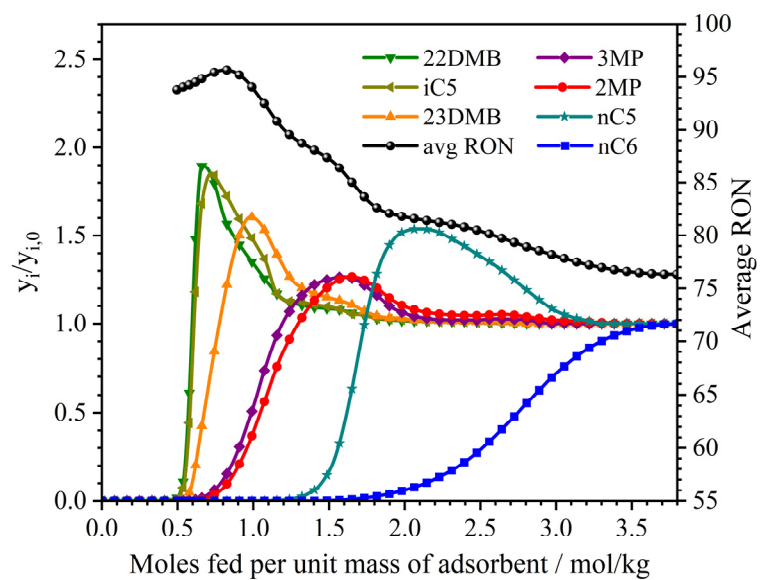


Figure S24. Experimental multicomponent breakthrough curves for an equimolar septenary mixture of C6 isomers in a mixed bed of shaped MOF MIL-160(Al) (70 wt%) and binder-free beads Zeolite 5A (30 wt%) at 473 K and 50 kPa.

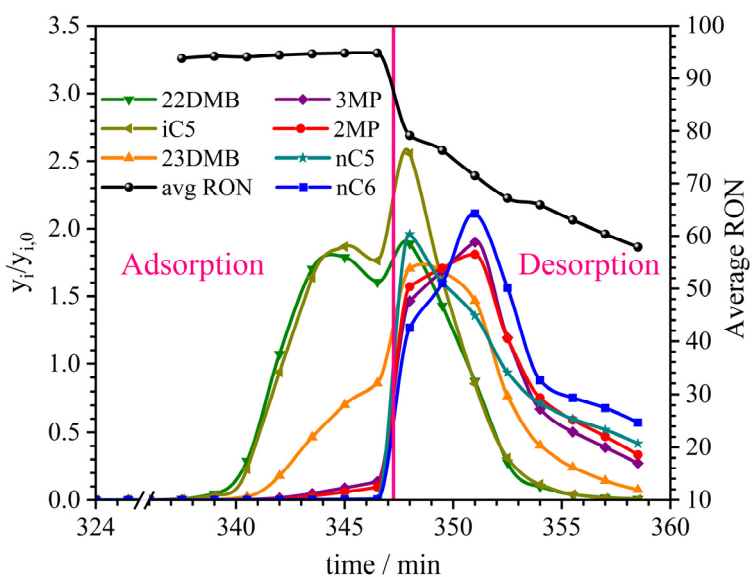


Figure S25. Experimental preliminary PSA test for an equimolar septenary mixture of C5/C6 isomers in a mixed bed of shaped MOF MIL-160(Al) (70%) and binder-free beads Zeolite 5A (30 wt%) at 473 K and 50.0 kPa. Steady-state effluent concentration.

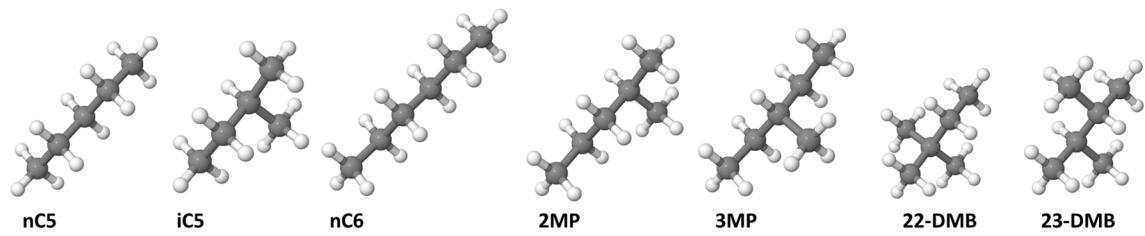


Figure S26. Molecular representation of the pentane/hexane isomers. Implicit hydrogen atoms are lumped onto the neighboring carbons and described with pseudo atoms CH3, CH2, CH and C according to TraPPE-UA potentials.

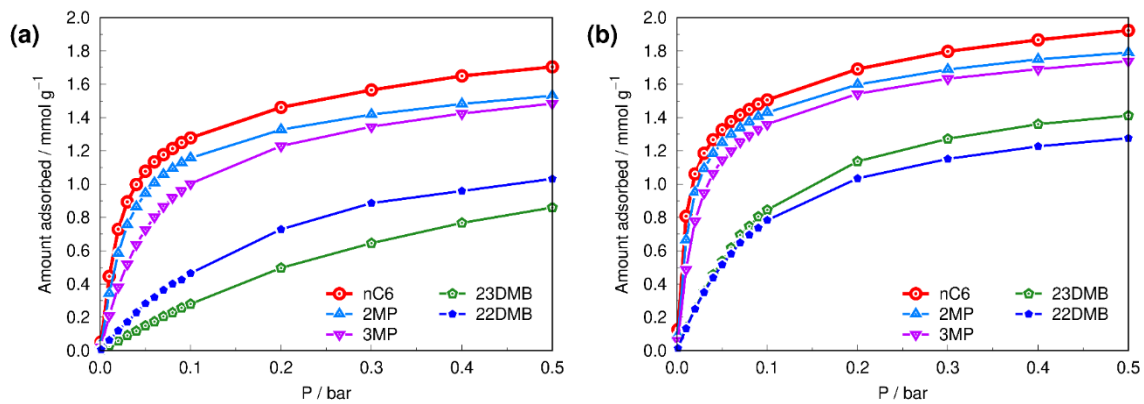


Figure S27. Simulated single component adsorption isotherms of hexane isomers in MIL-160 for the (a) pristine and (b) and 5° linker rotation obtained at 423 K.

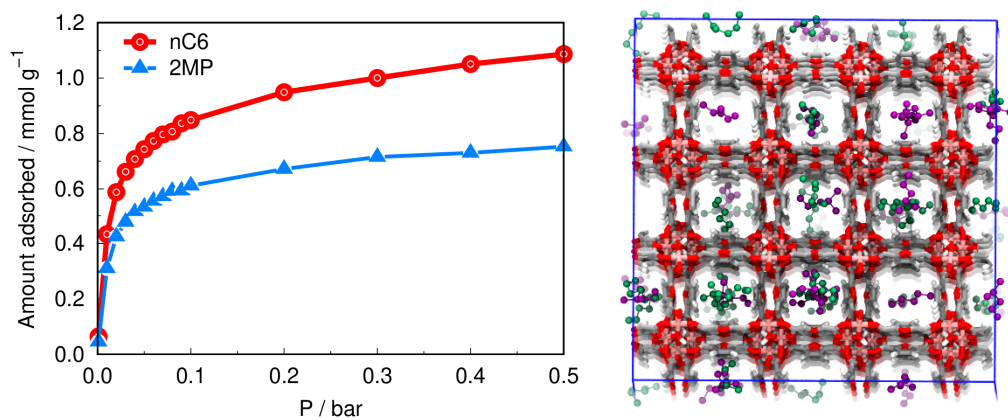


Figure S28. CBMC simulated co-adsorption isotherms of equimolar n-C6/2MP binary mixture for the MIL-160 with 5° tilted linkers at $T = 423$ K (left panel) and a snapshot of the adsorbed nC6 (green spheres) and 2MP (purple spheres) molecules at $P = 0.1$ bar within the channel of the MOF (right panel).

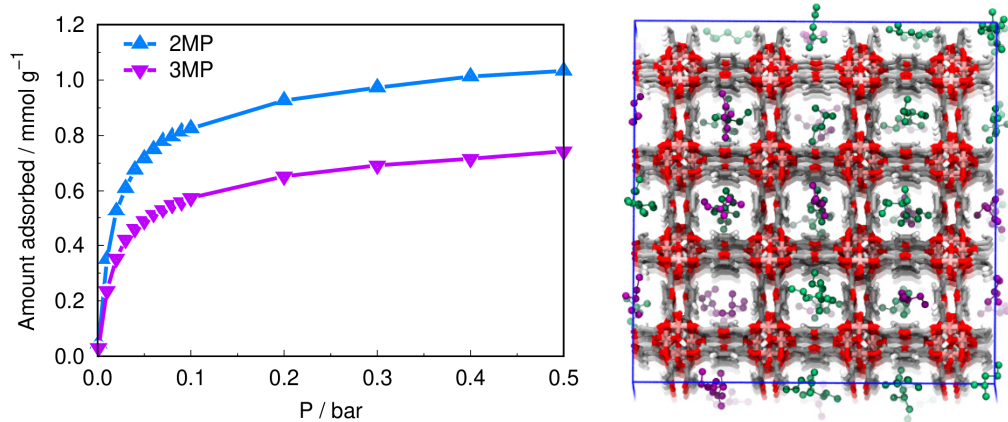


Figure S29. CBMC simulated co-adsorption isotherms of equimolar 2MP/3MP binary mixture for the MIL-160 with 5° tilted linkers at $T = 423$ K (left panel) and a snapshot of the adsorbed 2MP (green spheres) and 3MP (purple spheres) molecules at $P = 0.1$ bar within the channel of the MOF (right panel).

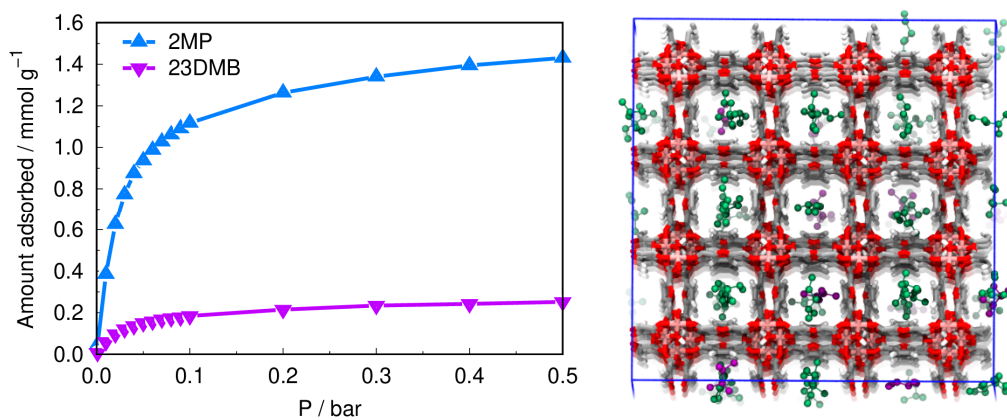


Figure S30. CBMC simulated co-adsorption isotherms of equimolar 2MP/23DMB binary mixture for the MIL-160 with 5° tilted linkers at $T = 423$ K (left panel) and a snapshot of the adsorbed 2MP (green spheres) and 23DMB (purple spheres) molecules at $P = 0.1$ bar within the channel of the MOF (right panel).

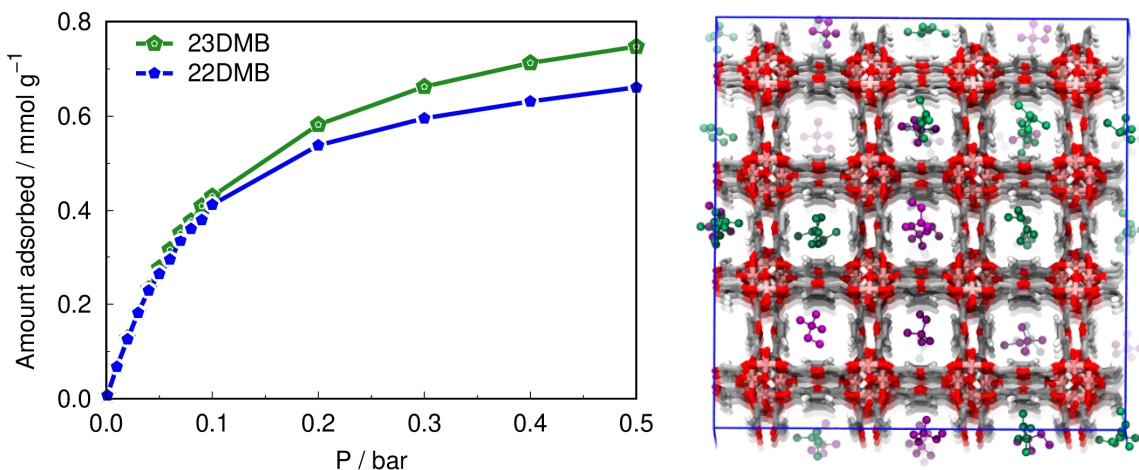


Figure S31. CBMC simulated co-adsorption isotherms of equimolar 22DMB/23DMB binary mixture for the MIL-160 with 5° tilted linkers at $T = 423$ K (left panel) and a snapshot of the adsorbed 22DMB (green spheres) and 23DMB (purple spheres) molecules at $P = 0.1$ bar within the channel of the MOF (right panel).

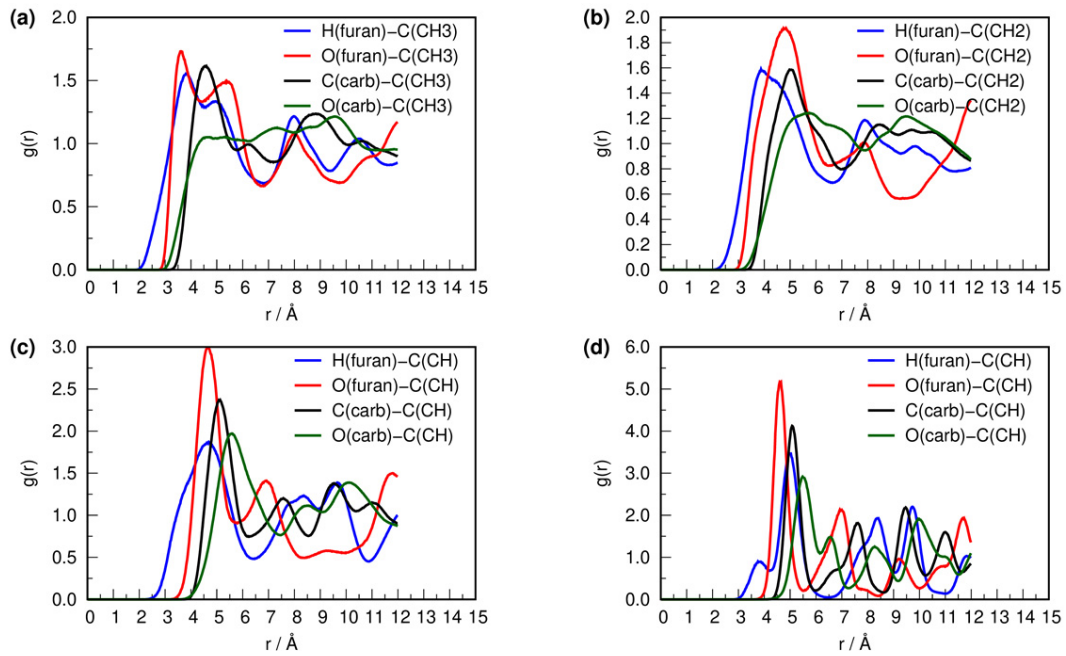


Figure S32. Intermolecular radial pair distribution functions of the (a) CH₃(UA), (b) CH₂(UA), (c) CH(UA) and (d) C of the hexane isomers with respect to MIL-160 framework atoms in the vicinity of the pore channel calculated for an equimolar quinary mixture at $T = 423$ K and $P = 0.1$ bar.

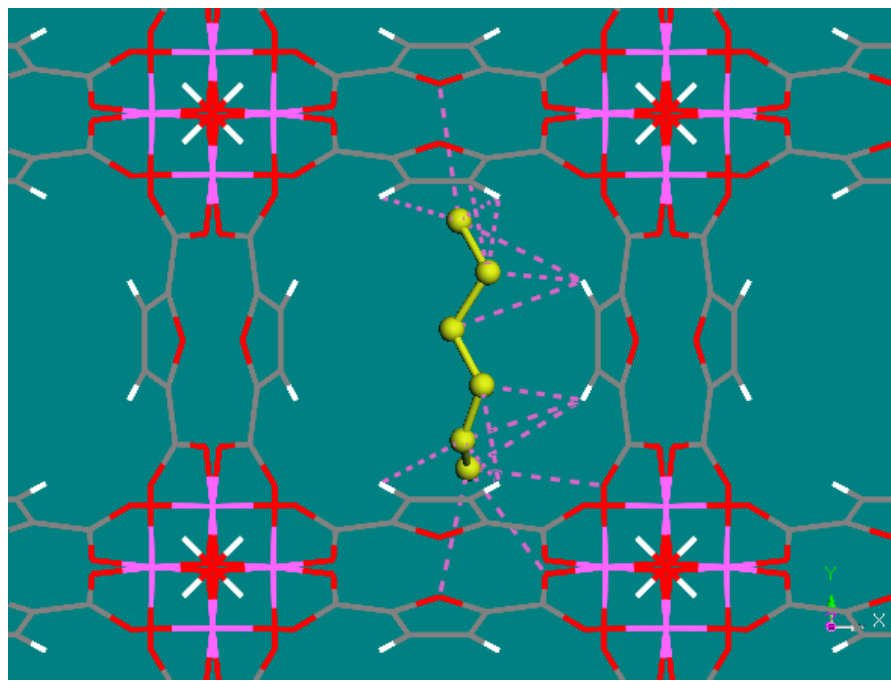


Figure S33. Illustration of a typical spatial arrangement and van der Waals close contacts (<3.5 Å) of a *n*-C₆ molecule with the MIL-160 pore walls taken from a representative adsorption snapshot derived from CBMC simulation performed for an equimolar quinary mixture of all C₆ isomers at $T = 423$ K and $P = 0.2$ bar.

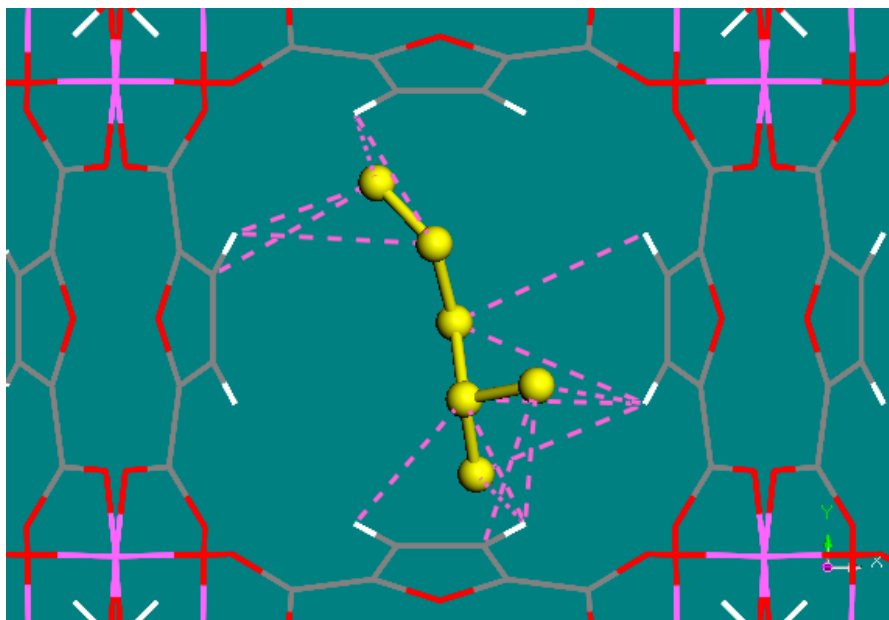


Figure S34. Illustration of a typical spatial arrangement and van der Waals close contacts (<3.5 Å) of a 2MP molecule with the MIL-160 pore walls taken from a representative adsorption snapshot derived from CBMC simulation performed for an equimolar quinary mixture of all C6 isomers at $T = 423$ K and $P = 0.2$ bar.

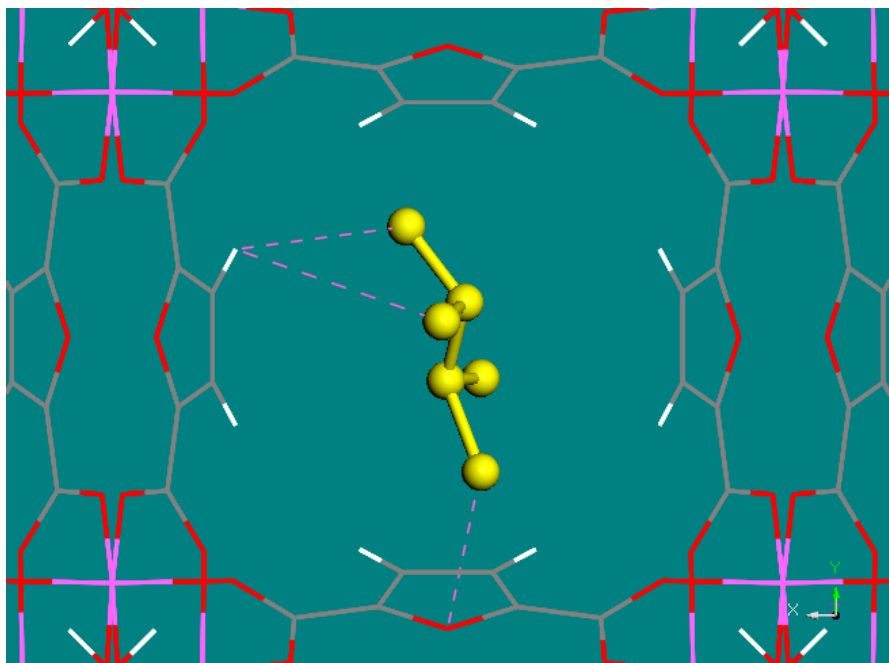


Figure S35. Illustration of a typical spatial arrangement and van der Waals close contacts (<3.5 Å) of a 23DMB molecule with the MIL-160 pore walls taken from a representative adsorption snapshot derived from CBMC simulation performed for an equimolar quinary mixture of all C6 isomers at $T = 423$ K and $P = 0.2$ bar.

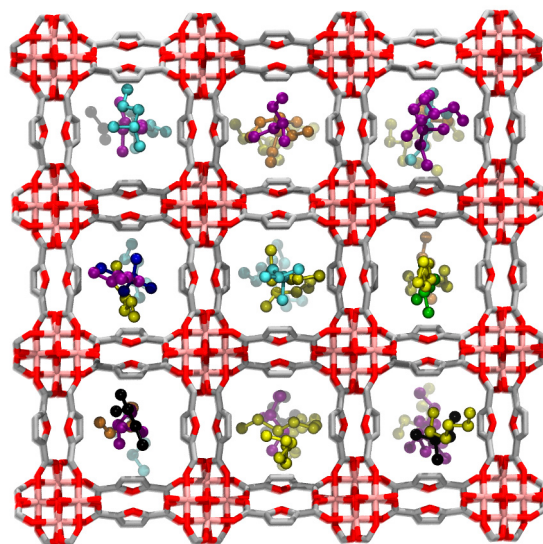


Figure S36. Illustration of CBMC simulated pore filling and spatial arrangement of all C5 and C6 isomers in the MOF channel obtained for an equimolar septenary mixture of C5/6 isomers at $P = 0.2$ bar and $T = 423$ K. Color codes: nC5 (orange spheres), iC5 (black spheres), nC6 (yellow spheres), 2MP (cyan spheres), 3MP (purple spheres), 23DMB (green spheres) and 22DMB (blue spheres), MOF framework atoms: Al (pink), Carbon (grey) and Oxygen (red), hydrogen atoms are omitted for clarity.

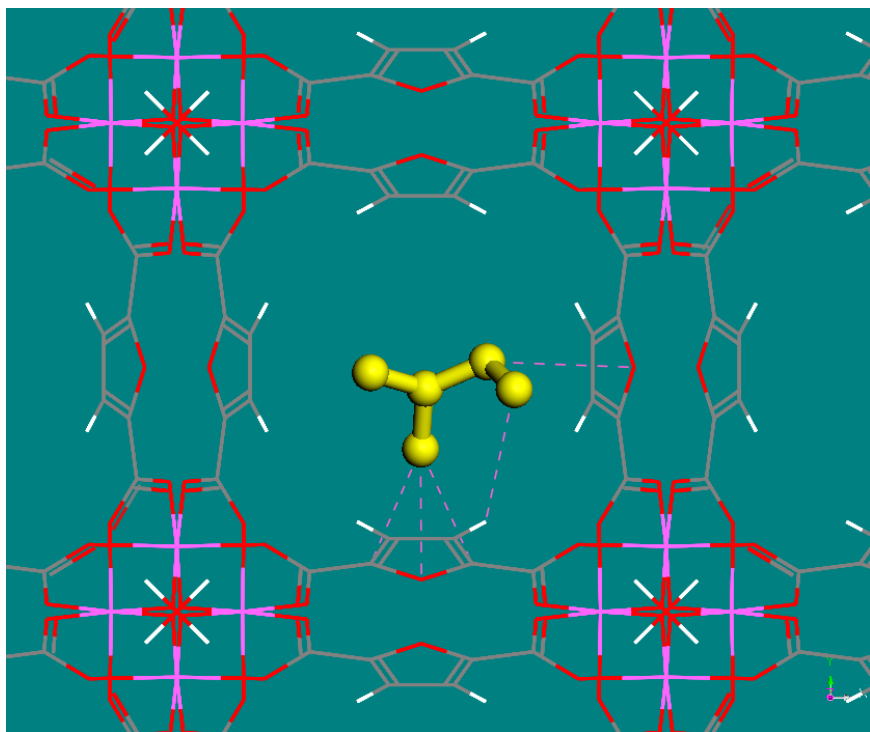


Figure S37. Illustration of a typical spatial arrangement and van der Waals close contacts (<3.5 Å) of a iC5 molecule with the MIL-160 pore walls taken from a representative adsorption snapshot derived from CBMC simulation performed for an equimolar septenary mixture of all C5 and C6 isomers at $T = 423$ K and $P = 0.2$ bar.

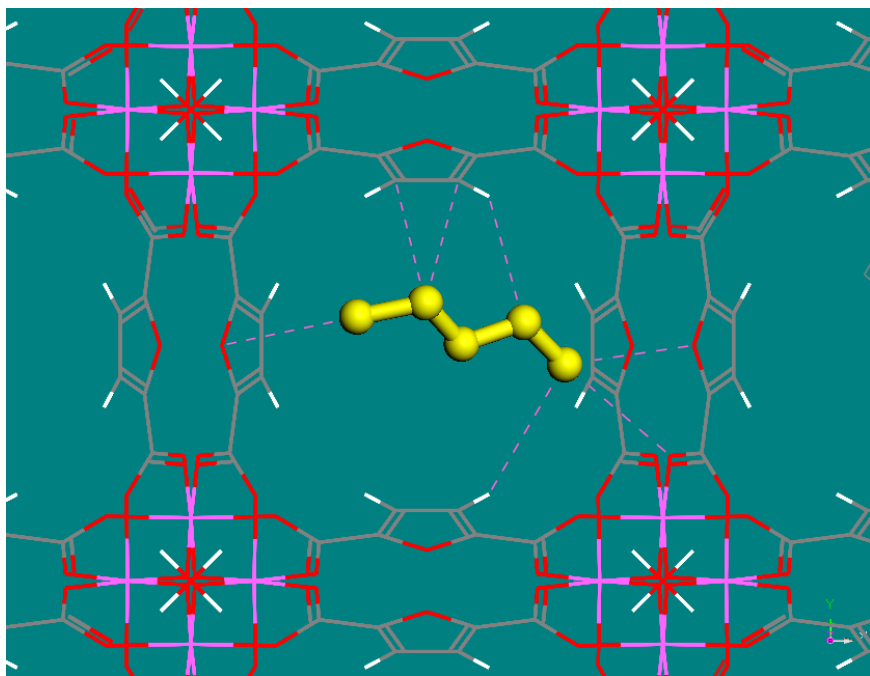


Figure S38. Illustration of a typical spatial arrangement and van der Waals close contacts (<3.5 Å) of a *n*-C5 molecule with the MIL-160 pore walls taken from a representative adsorption snapshot derived from CBMC simulation performed for an equimolar septenary mixture of all C5 and C6 isomers at $T = 423$ K and $P = 0.2$ bar.

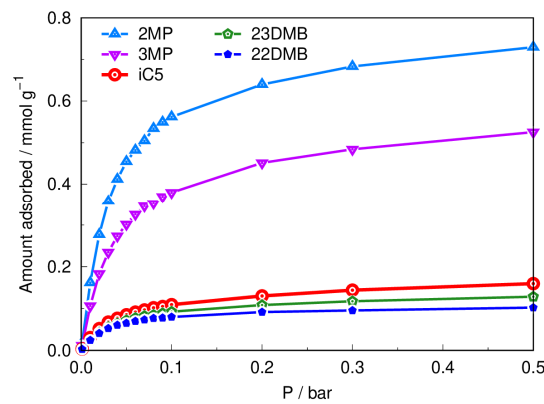


Figure S39. CBMC simulated co-adsorption isotherms of equimolar iC5/2MP/3MP/23DMB/22DMB mixture for the MIL-160 with 5° tilted linkers at $T = 423$ K.

Table S1. Textural properties of MIL-160(Al).

Adsorbent	S_{BET} ($\text{m}^2 \cdot \text{g}^{-1}$)	Median Pore (\AA)	Maximum pore volume ($\text{cm}^3 \cdot \text{g}^{-1}$)
MIL-160(Al)	1062	5.1	0.37

Table S2. Column, MFC's, and syringe characteristics for the experimental studies.

<i>Screening studies: powdered form</i>	
Column	0.0046 m internal diameter and 0.10 m length
MFC	MC-5SCCM-D/5M
Syringe	2.5 mL gastight syringe, 1002 TLL, PTFE Luer lock (Hamilton)
<i>Binary and ternary mixtures of C6 isomers: shaped form</i>	
Column	0.01 m internal diameter and 0.12 m length
MFC	MC-100SCCM-D/5M
Syringe	5.0 mL gastight syringe, 5MDF-LL-GT, PTFE Luer lock (SGE)
<i>Continuous cyclic experiments / quinary mixtures of C6 isomers: shaped form</i>	
Column	0.01 m internal diameter and 0.42 m length
MFC	MC-100SCCM-D/5M
Syringe	50 mL gastight syringe, 1050 TLL, PTFE luer lock (Hamilton)

Table S3. Molecular dimensions and research octane numbers of C5 and C6 alkanes.

C5/C6 Isomers	RON ¹¹	Molecular Shadow Length			Isomerization effluent (mol %) ⁵	Kinetic Diameter (Å) ^{14,15}
		X	Y	Z		
n-pentane (nC5)	61.7	9.1	4.5	4.0	25.9	4.3
iso-pentane (iC5)	93.5	-	-	-	32.0	5.0
2,2-dimethylbutane (22DMB)	94	8.0	6.7	5.9	3.7	6.2
2,3-dimethylbutane (23DMB)	105	7.8	6.7	5.3	2.9	5.6
2-methylpentane (2MP)	74.5	9.2	6.4	5.3	12.8	5.0
3-methylpentane (3MP)	75.5	9.3	6.2	5.2	8.5	5.0
n-hexane (nC6)	30	9.7	4.5	4.0	14.1	4.3

Table S4. Experimental conditions to measure multicomponent breakthrough curves for an equimolar quinary mixture of C6 isomers on powder MIL-160(Al).

Temp. (K)	Total isomers pressure (kPa)	Total Isomers flowrate STP ($\mu\text{mol} \cdot \text{min}^{-1}$)	Helium flowrate STP* ($\text{mL} \cdot \text{min}^{-1}$)	Mass of adsorbent (g)
373	10.0	16.20	3.31	
373	25.0	40.51	2.76	
373	50.0	44.03	1.00	
423	10.0	16.20	3.31	
423	25.0	14.68	1.00	0.4777
423	50.0	44.03	1.00	
473	10.0	16.20	3.31	
473	25.0	14.68	1.00	
473	50.0	44.03	1.00	

*STP: Standard Temperature and Pressure Conditions

Table S5. Experimental conditions to measure multicomponent breakthrough curves for an equimolar quinary mixture of hexane isomers on powder CAU-10(Al).

Temp. (K)	Total isomers pressure (kPa)	Total Isomers flowrate STP ($\mu\text{mol} \cdot \text{min}^{-1}$)	Helium flowrate STP ($\text{mL} \cdot \text{min}^{-1}$)	Mass of adsorbent (g)
423	50.0	81.01	1.84	0.4651

Table S6. Experimental conditions to measure multicomponent breakthrough curves for an equimolar quinary/septenary mixture of C5/C6 isomers on powder MIL-160(Al).

Temp. (K)	Total isomers pressure (kPa)	Total Isomers flowrate STP ($\mu\text{mol} \cdot \text{min}^{-1}$)	Helium flowrate STP ($\text{mL} \cdot \text{min}^{-1}$)	Mass of adsorbent (g)
373	50.0	81.01	1.84	
423	50.0	44.03	1.00	0.4777
473	50.0	44.03	1.00	

Table S7. Experimental conditions to measure pure component breakthrough curves of C6 isomers on shaped MIL-160(Al).

Temp. (K)	Total isomers pressure (kPa)	Total Isomers flowrate STP ($\mu\text{mol} \cdot \text{min}^{-1}$)	Helium flowrate STP ($\text{mL} \cdot \text{min}^{-1}$)	Mass of adsorbent (g)
373	2.5	12.15	10.76	
	5.0	24.31	10.49	
	10.0	48.61	9.94	
	20.0	97.21	8.83	
	30.0	145.82	7.73	
423	50.0	243.03	5.52	
	2.5	10.72	9.49	
	5.0	21.44	9.25	
	10.0	42.86	8.76	2.8107
	20.0	85.73	7.79	
473	30.0	128.59	6.81	
	50.0	214.32	4.87	
	2.5	9.58	8.49	
	5.0	19.17	8.27	
	10.0	38.33	7.83	
	20.0	76.67	6.96	
	30.0	115.00	6.09	
	50.0	191.67	4.35	

Table S8. Experimental conditions to measure multicomponent breakthrough curves for an equimolar binary/ternary mixture of C6 on shaped MIL-160(Al).

Temp. (K)	Total isomers pressure (kPa)	Total Isomers flowrate STP ($\mu\text{mol} \cdot \text{min}^{-1}$)	Helium flowrate STP ($\text{mL} \cdot \text{min}^{-1}$)	Mass of adsorbent (g)
423	50.0	81.01	1.84	4.3755

Table S9. Experimental conditions to measure multicomponent breakthrough curves for an equimolar quinary mixture of C6 isomers on shaped MIL-160(Al).

Temp. (K)	Total isomers pressure (kPa)	Total Isomers flowrate STP ($\mu\text{mol} \cdot \text{min}^{-1}$)	Helium flowrate STP (mL $\cdot \text{min}^{-1}$)	Mass of adsorbent (g)
423	50.0	281.29	7.0	16.54
473	50.0	251.57	6.2	

Table S10. Experimental conditions to measure multicomponent breakthrough curves for a septenary mixture of C5/C6 isomers on shaped MIL-160(Al) with an isomerization concentration¹⁶.

Temp. (K)	Total isomers pressure (kPa)	Total Isomers flowrate STP ($\mu\text{mol} \cdot \text{min}^{-1}$)	Helium flowrate STP ($\text{mL} \cdot \text{min}^{-1}$)	Mass of adsorbent (g)
423	50.0	81.01	1.84	5.2689

Table S11. Experimental conditions to measure multicomponent breakthrough curves for an equimolar septenary mixture of C5/C6 isomers in a mixed bed of shaped MOF MIL-160(Al) (70 wt%) and binder-free beads Zeolite 5A (30 wt%).

Temp. (K)	Total isomers pressure (kPa)	Total Isomers flowrate STP ($\mu\text{mol} \cdot \text{min}^{-1}$)	Helium flowrate STP ($\text{mL} \cdot \text{min}^{-1}$)	Mass of adsorbent (g)
423	50.0	562.58	13.9	18.29
473	50.0	503.13	12.5	

Table S12. Experimental conditions for preliminary PSA tests for an equimolar septenary mixture of C5/C6 isomers in a mixed bed of shaped MOF MIL-160(Al) (70 wt%) and binder-free beads Zeolite 5A (30 wt%).

Temp. (K)	Total isomers pressure (kPa)	Number of Cycles	Adsorption step time (min)	Desorption step time (min)	Total Duration (min)	Total Isomers flowrate STP ($\mu\text{mol} \cdot \text{min}^{-1}$)	Helium flowrate STP ($\text{mL} \cdot \text{min}^{-1}$)	Mass of adsorbent (g)
423	50.0	6	33	18	306	562.58	13.9	18.29
473	50.0	10	24	12	360	503.13	12.5	

Table S13. Intermolecular LJ-potential parameters for the C5 and C6 isomers.

Pseudo atom type	σ (Å)	ε/k_B (K)
CH ₃	3.75	98.0
CH ₂	3.95	46.0
CH	4.68	10.0
C	6.40	0.5

Table S14. Intermolecular LJ Potential parameters for the MIL-160(Al) framework atoms.

Atom type	σ (Å)	ϵ/k_B (K)
H	2.571	0
C	52.839	4.008
O	30.194	3.118
Al	4.008	0

Table S15. Henry's constants (K_H) of hexane and pentane isomers in MIL-160(Al) at 423 K.

K_H (mol/kg/Pa)	
<i>n</i> -C6	1.18e-03
2MP	8.26e-04
3MP	6.11e-04
<i>n</i> -C5	3.80e-04
<i>i</i> -C5	1.74e-04
23DMB	1.36e-04
22DMB	1.34e-04

REFERENCES

1. Cadiau, A. *et al.* Design of Hydrophilic Metal Organic Framework Water Adsorbents for Heat Reallocation. *Adv. Mater.* **27**, 4775–4780 (2015).
2. Thommes, M. *et al.* Physisorption of Gases, with Special Reference to the Evaluation of Surface Area and Pore Size Distribution (IUPAC Technical Report). *Pure Appl. Chem.* **87**, 1051–1069 (2015).
3. Chang, J. S. *et al.* Adsorbents Comprising Organic-Inorganic Hybrid Nanoporous Materials for Sorption of Water or Alcohol and use Thereof. (2016).
4. Henrique, A., Rodrigues, A. E. & Silva, J. A. C. Separation of Hexane Isomers in ZIF-8 by Fixed Bed Adsorption. *Ind. Eng. Chem. Res.* **58**, 378–394 (2019).
5. Holcombe, T. C., Sager, T. C., Volles, W. K. & Zarchy, A. S. Isomerization Process. U.S. Patent 4,929,799. (1990).
6. Henrique, A. *et al.* Hexane isomers separation on an isoreticular series of microporous Zr carboxylate metal organic frameworks. *J. Mater. Chem. A* **8**, 17780–17789 (2020).
7. Dubbeldam, D., Calero, S., Ellis, D. E. & Snurr, R. Q. RASPA: Molecular simulation software for adsorption and diffusion in flexible nanoporous materials. *Mol. Simul.* **42**, 81–101 (2016).
8. Martin, M. G. & Siepmann, J. I. Transferable potentials for phase equilibria. 1. United-atom description of n-alkanes. *J. Phys. Chem. B* **102**, 2569–2577 (1998).
9. Martin, M. G. & Siepmann, J. I. Novel configurational-bias Monte Carlo method for branched molecules. Transferable potentials for phase equilibria. 2. United-atom description of branched alkanes. *J. Phys. Chem. B* **103**, 4508–4517 (1999).
10. Rappé, A. K., Casewit, C. J., Colwell, K. S., Goddard, W. A. & Skiff, W. M. UFF, a Full Periodic Table Force Field for Molecular Mechanisms and Molecular Dynamics Simulations. *J. Am. Chem. Soc.* **114**, 10024–10035 (1992).

11. Herm, Z. R. *et al.* Separation of Hexane Isomers in a Metal-Organic Framework with Triangular Channels. *Science*. **340**, 960–964 (2013).
12. Peralta, D., Chaplain, G., Simon-Masseron, A., Barthelet, K. & Pirngruber, G. D. Separation of C6 Paraffins Using Zeolitic Imidazolate Frameworks: Comparison with Zeolite 5A. *Ind. Eng. Chem. Res.* **51**, 4692–4702 (2012).
13. Webster, C. E., Drago, R. S. & Zerner, M. C. Molecular dimensions for adsorptives. *J. Am. Chem. Soc.* **120**, 5509–5516 (1998).
14. Maloncy, M. L., Gora, L., Jansen, J. C. & Maschmeyer, T. Conceptual Processes for Zeolite Membrane Based Hydroisomerization of Light Alkanes. *Ars Sep. Acta* **2**, 18–28 (2003).
15. Tantekin-Ersolmaz, S. B., Şenorkyan, L., Kalaonra, N., Tatlier, M. & Erdem-Şenatalar, A. n-Pentane/i-Pentane separation by using zeolite-PDMS mixed matrix membranes. *J. Memb. Sci.* **189**, 59–67 (2001).
16. Holcombe, T. C., Sager, T. C., Volles, K. & Zarchy, A. S. Isomerization Process. (1990).